

1-1-2011

Stabilization of oil-in-water emulsions via soy protein and soy soluble polysaccharide interactions

Tu Tran
Ryerson University

Follow this and additional works at: <http://digitalcommons.ryerson.ca/dissertations>

 Part of the [Cellular and Molecular Physiology Commons](#)

Recommended Citation

Tran, Tu, "Stabilization of oil-in-water emulsions via soy protein and soy soluble polysaccharide interactions" (2011). *Theses and dissertations*. Paper 1650.

This Thesis is brought to you for free and open access by Digital Commons @ Ryerson. It has been accepted for inclusion in Theses and dissertations by an authorized administrator of Digital Commons @ Ryerson. For more information, please contact bcameron@ryerson.ca.

Stabilization of Oil-in-Water Emulsions *via* Soy Protein and Soy Soluble Polysaccharide Interactions

by

Tu Tran

B.Sc., Ryerson University, Toronto, Canada, 2008

A thesis presented to Ryerson University

in partial fulfillment of the

requirements for the degree of

Master of Science

in the program of

Molecular Science

Toronto, Ontario, Canada, 2011

©Copyright by Tu Tran 2011

I hereby declare that I am the sole author of this thesis.

I authorize Ryerson University to lend this thesis to other institutions or individuals for the purpose of scholarly research.

I further authorize Ryerson University to reproduce this thesis by photocopying or by other means, in total or in part, at the request of other institutions or individuals for the purpose of scholarly research.

Stabilization of oil-in-water emulsions *via* soy protein and soy soluble polysaccharide interactions

Tu Tran

Ryerson University

Master of Science

in the program of

Molecular Science

2011

Abstract

The stabilizing behaviour of soluble soy polysaccharide (SSPS) on acidified dispersions of soy protein isolate (SPI) and SPI-stabilized emulsions was studied. SPI and SSPS suspensions were characterized via light scattering, surface charge measurement, turbidity, sedimentation analysis, and light microscopy. At acidic pH (pH 6-3), it was found the addition of at least 0.25 wt% SSPS was required to stabilize 0.75 wt% SPI suspensions against aggregation and phase separation, likely *via* steric repulsion. The mechanism of SPI-SSPS interaction was shown to be electrostatic in nature by testing the effects of increased ionic strength of the suspensions. The stabilizing effect of SSPS on SPI was then applied to 5% oil-in-water emulsions. The presence of SSPS stabilized the emulsions against droplet size increases and phase separation over time. Overall, these results demonstrated that it was possible for SSPS to stabilize SPI suspensions and that SPI-SSPS interactions may be used as a tool to stabilize O/W emulsions.

Acknowledgements

I would first like to thank my supervisor, Dr. D errick Rousseau, for his guidance, insight, patience, and generosity throughout my Master’s studies. He was always eager to help and provided many great ideas that have helped to shape this thesis. He was very understanding during some difficult times and for that I will be forever grateful.

I would also like to thank my thesis committee members, Drs. Darrick Heyd and Stephen Wylie, who provided valuable insight into my work.

I thank Dr McWilliams, who was kind enough to volunteer his time for my defense.

For their help in various characterization techniques, I would like to thank:

- Dr. John Marshall (Protein characterization)
- Dr. Supratim Ghosh (High-pressure valve homogenizer, microscopy)
- Dr. Tejas Patel (Turbiscan)
- Ms. Moumita Ray and Dr. Renuka Gupta (Particle size and zeta potential measurements)

I would like to thank all of my lab colleagues, especially Natasha, Muhammad, Moumita, Lanny, Samira, and Tejas for their helpful discussions and friendships during my research. They have made my Master’s experience a most enjoyable one.

I would like to say a special thank you to my family, especially my mom and dad, for always being there to support me and encourage me.

Finally, I would like to thank my wife, Yasmin, for her patience, love, and support. You are the one that kept me going. Thank you for believing in me.

Tu Tran

Table of Contents

Abstract	iii
Acknowledgements	iv
List of tables.....	viii
List of figures.....	ix
Acronyms and abbreviations.....	xii
List of symbols.....	xiii
Chapter 1 - Introduction.....	1
1.0 Introduction.....	1
1.1 Colloids and interfaces	1
1.2 Fundamentals of colloidal systems.....	2
1.2.1 DLVO theory and its limitations	2
1.3 Instability of emulsion systems.....	5
1.3.1 Sedimentation and creaming.....	6
1.3.2 Flocculation and aggregation.....	7
1.3.3 Coalescence	8
1.3.4 Compatibility of biopolymers	10
1.4 Improving the stability of emulsion systems.....	12
1.5 Thesis objectives	12
1.6 Hypotheses.....	13
1.7 Methodology and approach	13
Chapter 2 - Literature Review.....	14
2.0 Introduction.....	14
2.1 Proteins as surfactants.....	14
2.2 Polysaccharides as emulsion stabilizers.....	19
2.3 Protein-polysaccharide interactions for suspension and emulsion stabilization	21

Chapter 3 – Experimental methods	23
3.0 Introduction.....	23
3.1 Protein and polysaccharide suspension preparation.....	23
3.2 Emulsion preparation.....	24
3.3 Particle/droplet size determination.....	24
3.4 Surface charge determination.....	26
3.5 Turbidity analysis	28
3.6 Light microscopy	29
3.8 Data analysis	30
Chapter 4 – Stabilization of oil-in-water emulsions <i>via</i> soy protein and soy soluble polysaccharide interactions	31
4.1 Introduction.....	31
4.2 Materials and methods.....	31
4.2.1 Materials.....	31
4.2.2 Methods	31
4.2.2.1 Preparation of SPI and SSPS stock suspensions.....	31
4.2.2.2 Preparation of mixed SPI and SSPS suspensions	32
4.2.2.3 Preparation of SPI-SSPS-stabilized emulsions.....	32
4.3 Characterization of SPI and SSPS suspensions and emulsions	32
4.3.1 SDS-PAGE analysis.....	32
4.3.2 Particle/droplet size measurement	33
4.3.3 Surface charge measurement	33
4.3.4 Turbidity and sedimentation/creaming	34
4.3.5 Inverted light microscopy	34
4.4 Results and Discussion.....	35
4.4.1 Characterization of SPI and SSPS suspensions	35
4.4.2 Characterization of SPI-SSPS-stabilized emulsions.....	53
4.5 Conclusions	62

Chapter 5 - Overall Conclusions	63
Chapter 6 - Future Studies	64
Chapter 7 - References	65

List of Tables

Table 4.1	The effect of 1 wt% NaCl on the average particle sizes of 0.75 wt% SPI + 0.75 wt% SSPS suspensions at pH 3-6.
Table 4.2	Evolution of clearing rates for 0.75 wt% SPI-stabilized emulsions with various concentrations of SSPS.
Table 4.3	Evolution of pre-creaming rates for 0.75 wt% SPI-stabilized emulsions with various concentrations of SSPS.

List of Figures

Figure 1.1	Schematic of DLVO theory for the potential energies of interaction between colloidal particles as a function of separation distance.
Figure 1.2	Schematic of the electrical double layer around a positively-charged particle.
Figure 1.3	Schematic of common mechanisms for the destabilization of typical food-related O/W or W/O emulsions.
Figure 1.4	Common and Newton black films between protein-stabilized oil droplets.
Figure 1.5	Schematic of the process of coalescence.
Figure 1.6	Schematic for the different types of possible interactions between proteins and polysaccharides in aqueous suspensions.
Figure 2.1	The structure of glycinin and β -conglycinin.
Figure 2.2	pH-solubility profile of SPI isolate in water.
Figure 2.3	The structure of SSPS.
Figure 3.1	Schematic of a Polytron PT 10-35 rotor-stator bench top homogenizer.
Figure 3.2	Schematic of the high pressure emulsification process in an APV 1000 valve homogenizer.
Figure 3.3	Schematic of the Malvern Mastersizer 2000 operating principle.
Figure 3.4	A sample particle size distribution of an SPI-stabilized oil-in-water emulsion.

Figure 3.5	Schematic representation of an electric double layer depicting the surface of shear.
Figure 3.6	Schematic representation of the Turbiscan's operating principle.
Figure 4.1	SDS-PAGE gel of SPI and molecular weight standards.
Figure 4.2	The effect of pH on the particle size distributions of 0.75 wt% SPI-stabilized suspensions with varying concentrations of SSPS.
Figure 4.3	The effect of pH on the zeta potential of 0.75 wt% SPI suspensions with varying concentrations of SSPS.
Figure 4.4	The effect of pH on the sedimentation of 0.75 wt% SPI control suspensions versus 0.75 wt% SPI + 0.25 wt% SSPS suspensions.
Figure 4.5	The effect of pH on the transmission profiles of 0.75 wt% SPI suspensions with varying concentrations of SSPS.
Figure 4.6	The effect of pH on the transmission of 0.75 wt% SPI suspensions with varying concentrations of SSPS.
Figure 4.7	Sedimentation of 0.75 wt% SPI control suspensions over time at various pHs.
Figure 4.8	The effect of 1 wt% NaCl on the sedimentation of 0.75 wt% SPI suspensions after 24 hours.
Figure 4.9	The effect of 1 wt% NaCl on the sedimentation of 0.75 wt% SPI suspensions after 14 days.
Figure 4.10	The possible effect of NaCl on interactions between SPI-SSPS complexes.
Figure 4.11	The effect of ionic strength on the particle size distributions of 0.75 wt% SPI + 0.75 wt% SSPS suspensions at various pHs.
Figure 4.12	The effect of pH on the microstructure of 0.75 wt% SPI suspensions.

- Figure 4.13** The effect of 1 wt% NaCl on the microstructure of 0.75 wt% SPI + 0.75 wt% SSPS suspensions at various pHs.
- Figure 4.14** The effect of pH on the droplet size distributions of 0.75 wt% SPI-stabilized emulsions with and without SSPS.
- Figure 4.15** The evolution of average droplet sizes over time for 0.75 wt% SPI-stabilized emulsions with varying concentrations of SSPS.
- Figure 4.16** The effect of pH on the creaming of 0.75 wt% SPI-stabilized emulsions with and without SSPS.
- Figure 4.17** The effect of pH on the backscattering profiles of 0.75 wt% SPI-stabilized emulsions with and without SSPS.
- Figure 4.18** The evolution of the backscattering profile of a 0.75 wt% SPI + 0.75 wt% SSPS emulsion at pH 8 over time.
- Figure 4.19** The effect of pH on the microstructure of 0.75 wt% SPI-stabilized emulsions with and without SSPS.

Acronyms and Abbreviations

(In alphabetical order)

CBF	Common black film
CCD	Charge-coupled device
DLVO theory	Derjaguin, Landau, Verwey, and Overbeek theory
DSD	Droplet size distribution
HMP	High methoxyl pectin
IEP	Isoelectric point
NBF	Newton black film
O/W	Oil-in-water emulsion
O/W/O	Oil-in-water-in-oil emulsion
PSD	Particle size distribution
SPI	Soy protein isolate
SSPS	Soy soluble polysaccharide
W/O	Water-in-oil emulsion
W/O/W	Water-in-oil-in-water emulsion

List of Symbols (In alphabetical order)

A	Acidic subunit of glycinin
B	Basic subunit of glycinin
c	Sample concentration
D(3,2)	Surface-weighted average particle or droplet size
D(4,3)	Volume-weighted average particle or droplet size
dx/dt	Terminal velocity of a particle undergoing sedimentation or creaming
$F_{\text{suspension}}$	Percent of suspension layer
g	Gravitational constant
H_0	Interparticle distance
$h_{\text{suspension}}$	Height of suspension layer
h_{total}	Total height of a suspension sample
I	Intensity of scattered light
I_0	Intensity of incident light
I_d	Intensity of light at a distance d from a scattering particle
I_t	Intensity of transmitted light
	Path length through a sample
p	Probability statistic
r	Particle radius
T_r	Transmission of light through a sample

V_A	London-van der Waals attractive interaction energy
V_{DL}	Electrical double layer repulsive interaction energy
V_{max}	Primary energy barrier for particle/droplet interaction
V_R	Electrostatic repulsive interaction energy
V_T	Total interaction potential
x	Distance of scattered light from a particle
y	Ratio of the refractive index of a dispersed particle or droplet relative to the medium
α	Subunit of β -conglycinin
α'	Subunit of β -conglycinin
β	Subunit of β -conglycinin
ΔBS	Difference in backscattering
ϵ	Dielectric constant of a medium
ζ	Zeta potential
η	Viscosity
λ	Wavelength of light
μ_e	Electrophoretic mobility
ρ	Density
τ	Turbidity

Chapter 1 – Introduction

1.0 Introduction

An extensive amount of work has been performed on the characterization of oil-in-water emulsions stabilized by proteins, polysaccharides and protein-polysaccharide interactions, but little work has been performed on the characterization of such emulsions stabilized by soy protein isolate (SPI) and soy soluble polysaccharide (SSPS). This thesis focuses on the elucidation of the mechanism of soy-based protein-polysaccharide interactions and their role in oil-in-water emulsion formation and stability. The present chapter briefly highlights some of the fundamentals of colloid stability and how these apply to emulsions and their kinetic stability.

1.1 Colloids and interfaces

A colloid is a gas, liquid or solid dispersed throughout another substance with dimensions between 1 and 1000 nm [1]. Due to their small size, colloids have a high surface-area-to-volume, making them susceptible to strong inter-particle forces. These forces can be attractive, such as London-van der Waals forces, or they can be repulsive, such as electrostatic repulsion forces. Together, these dictate the properties of colloidal dispersions [2].

Colloidal dispersions can be simple and consist of only two phases, such as clay particles in water, or complex systems with multiple components, such as exfoliating facial scrubs [1]. These same governing principles can also be applied to emulsions which are suspensions of two immiscible liquids with one dispersed in the other [2]. Emulsions can be classified as oil-in-water (O/W), water-in-oil (W/O), oil-in-water-in-oil (O/W/O), or water-in-oil-in-water (W/O/W). In O/W emulsions, which are the topic of the present thesis, oil droplets are suspended in a continuous aqueous phase. Food-grade examples of such emulsions include mayonnaise, whipped cream, and ice cream. Water-in-oil emulsions consist of water droplets suspended a continuous oil phase; examples include butter, margarine, and other tablespreads. O/W/O emulsions consist of oil droplets contained within water droplets which are themselves dispersed in an external oil phase whereas W/O/W emulsions are water droplets inside oil droplets dispersed in an aqueous phase. Examples of O/W/O and W/O/W emulsions include confectionery spreads and pharmaceutical drug delivery systems, respectively [1, 3-5].

Emulsions are inherently thermodynamically unstable due to the interfacial tension that exists between the dispersed and continuous phases, but they can be made kinetically stable *via* the addition of surfactants, which reduce interfacial tension [1, 5]. Input of energy *via* homogenization or mixing, along with the use of surfactants, can reduce droplet sizes to below 1 micron and slow down destabilization processes such as flocculation and coalescence, which are responsible for phase separation.

Surfactants, by definition, are surface-active molecules that contain both hydrophobic and hydrophilic moieties. This allows them to adsorb to oil-water interfaces and reduce interfacial tension, resulting in greater emulsion stability. Surfactants can also stabilize emulsions *via* electrostatic and/or steric repulsion, as described later [5]. Key types of surfactants include low molecular weight surfactants, such as polysorbates and lecithins, and biopolymers, such as proteins and polysaccharides.

Proteins are widely-used emulsifiers not only due to their interfacial tension-lowering capacity, but also given their ability to alter the rheological properties of oil-water interfaces where they can form gel-like films that resist destabilization *via* electrostatic and/or steric repulsion [6]. Polysaccharides may also be used to improve emulsion stability, either by increasing the viscosity of the continuous phase, lowering surface or interfacial tension, or by interacting with proteins at the droplet interface to form multi-layer coatings. [7]. This thesis focuses on the use of proteins and polysaccharides to form and stabilize O/W emulsions.

1.2 Fundamentals of colloidal systems

1.2.1 DLVO theory and its limitations

The DLVO theory (named after Derjaguin, Landau, Verwey, and Overbeek) states that the stability of a colloidal dispersion depends on the total interaction potential close to the surface of the dispersed phase [2]. This total interaction potential V_T is the sum of the repulsive electrostatic interaction energy V_R and the attractive London-van der Waals energy V_A (Equation 1.1):

Eqn. 1.1

Using the DLVO theory, one can estimate the changes in energy as two particles approach each other (Fig. 1.1):

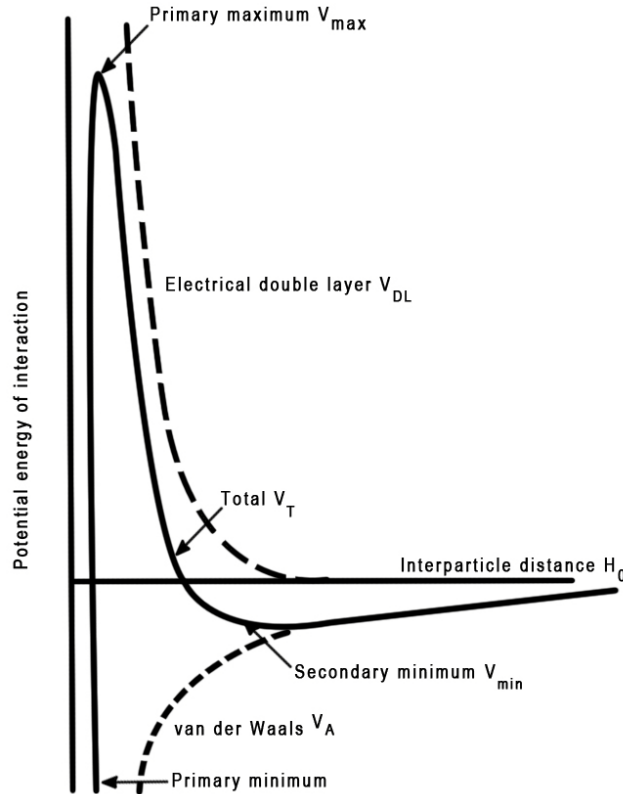


Figure 1.1 – Potential energies of interaction between colloidal particles as a function of separation distance (H_0): electrical double layers (repulsive interaction energy) V_{DL} ; London-van der Waals dispersion forces (attractive interaction energy) V_A ; and total interaction V_T are shown (adapted from [1]).

Repulsive energy due to electrostatic repulsion increases exponentially with decreasing interparticle distance H_0 , whereas attractive London-van der Waals energy increases with decreasing H_0 . Attractive forces predominate at large and small interparticle distances, resulting in two energy minima: the secondary and primary minima, respectively. The secondary energy minimum can promote loose, easily reversible flocculation if its magnitude is no greater than 10 kT. The primary minimum represents irreversibly flocculated particles after they have overcome the primary energy maximum due to the repulsive interaction energy barrier (V_{max}) (Fig. 1.1). This can occur if the particles approach each other with kinetic energies ≥ 15 kT. At intermediate and small interparticle distances known as Born distances, where electron clouds of molecules overlap, repulsive forces dominate [1]. These forces are due to electrostatic repulsion between the particles' electric double layers (Fig. 1.2). Electrostatic repulsion, and therefore the energy barrier, depends on electrolyte content while attraction energy remains constant [1]. This allows one to control the stability of colloidal systems by changing the ionic strength of the suspension [1, 2]. Increasing the ionic strength of a suspension causes increased binding of counterions to the colloid surface which

results in a decrease in surface potential and the effective radius the double layer (double layer compression) [5, 8]. This results in a reduction of the electrostatic repulsion energy barrier (V_{DL}).

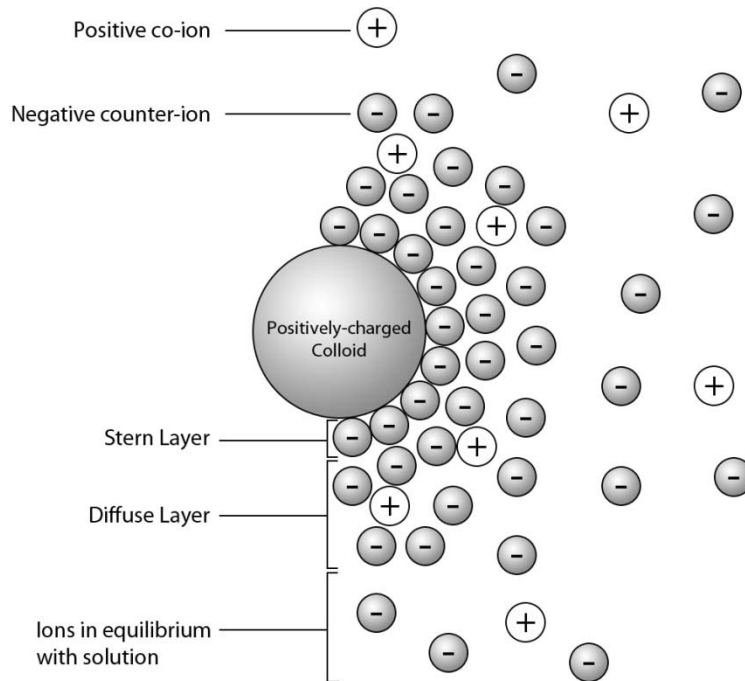


Figure 1.2 – Schematic of the electrical double layer around a positively-charged particle (adapted from [1]).

The DLVO theory only accounts for repulsive forces due to electrostatic repulsion as a consequence of interacting electrical double layers and attractive forces due to London-van der Waals interactions. As discussed below, other attractive and repulsive forces may play a significant part in a colloidal dispersion's stability. These include hydrophobic interactions, hydration effects, and steric repulsion.

Hydrophobic interactions are attractive in nature and are caused by the exposure of hydrophobic surfaces to water. Normally, water molecules undergo hydrogen bonding and are highly organized [1]. The introduction of a hydrophobic surface disrupts this structuring because there are no polar groups on the hydrophobic surface to hydrogen bond with the water molecules. As a consequence, water molecules try to minimize contact with these surfaces. This leads to hydrophobic bonding between hydrophobic surfaces in order to minimize contact with water [1, 8].

Hydration effects may cause repulsive forces between colloidal particles or droplets. The behaviour of water near a particle or droplet's surface is usually different than that of bulk water [8]. This results in short-range hydration effects that cause increased repulsion between two approaching particles because ions at the particle/droplet surface must lose their water of hydration before interaction can occur [1, 8]. Hydration effects become significant at ionic strengths ≥ 1 mM and increase with the degree of hydration. These forces are appreciable relative to the range of electrostatic double layer repulsion and may have a significant role in colloidal stability, especially at higher ionic strengths when hydrated metal ions may adsorb onto charged surfaces [1, 8].

Steric repulsion may occur when a considerable amount of adsorbed material extends out from the surface of a particle/droplet. For example, with polymer or protein-covered oil droplets in emulsions, hydrophilic moieties may result in a 'hairy' layer around droplets [5]. When two particles or droplets approach each other, the interaction of the hydrophilic chains may cause structuring of the aqueous phase, resulting in a decrease in entropy. This results in a short-range, volume-limited repulsive force that leads to steric stabilization. The degree of steric stabilization depends on the thickness of the adsorbed layer relative to the size of the particles or droplets. Steric stabilization by a thick, impermeable adsorbed layer may impart a salt tolerance and can stabilize colloidal suspensions even at high salt concentrations [1].

1.3 Instability of emulsion systems

Emulsions are used in a variety of food applications such as ice cream, salad dressings, mayonnaise, table spreads, processed cheese, and even meat substitutes [5, 6, 9]. This is because they confer such food products a desirable taste, texture and/or mouthfeel. These properties as well as an emulsion's kinetic stability strongly depend on composition, including the type of oil used for the oil phase, the type of surfactant(s) used, the pH, and the ionic strength (*i.e.*, presence of salt). Emulsion processing (namely homogenization and thermal treatments) will also impact emulsion properties and stability. The key means of emulsion breakdown include sedimentation/creaming, flocculation, and coalescence (Fig. 1.3).

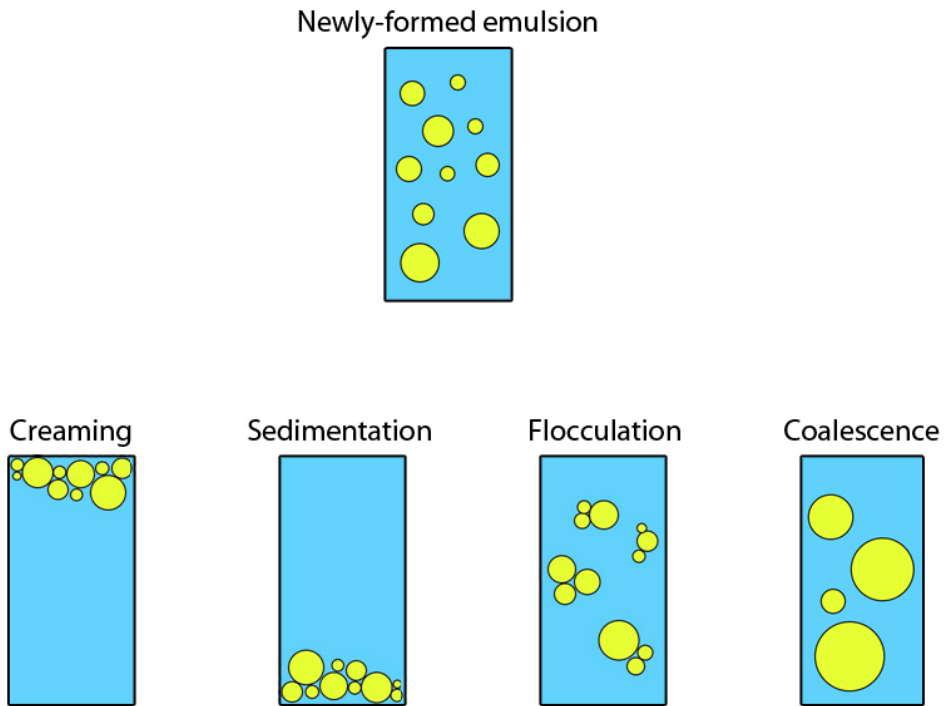


Figure 1.3 – Common mechanisms for the destabilization of typical food-related O/W or W/O emulsions.

1.3.1 Sedimentation and Creaming

Over time, particles or droplets of a colloidal suspension will settle to the bottom or rise to the top of a sample if their density is greater or less than that of the continuous phase, respectively (Fig. 1.3). The former phenomenon is known as sedimentation and the latter as creaming. Whether a particle or droplet undergoes sedimentation or creaming depends on its size, density, the density of the continuous phase, and the viscosity of the continuous phase. Stoke’s law provides an estimate of the rate of sedimentation and creaming:

$$v = \frac{2r^2(\rho_2 - \rho_1)g}{9\eta}$$

Eqn. 1.2

where dx/dt is the terminal velocity of the particle/droplet, r is the particle/droplet radius, ρ_1 is the density of the continuous phase, ρ_2 is the density of the particle/droplet, g is the gravitational

constant, and η is the viscosity of the continuous phase [1]. Equation 1.2 accounts for the three main forces affecting the sedimentation or creaming of particles/droplets: gravity, friction, and buoyancy. The effect of gravity is related to particle size with larger particles resulting in increased sedimentation/creaming rates. This explains why flocculated and aggregated particles/droplets, which have larger effective radii, sediment faster than individual particles/droplets. Friction and buoyancy are affected by the properties of the suspension or dispersion – decreasing the viscosity of the continuous phase reduces the force of friction acting on the dispersed particles/droplets, leading to increased sedimentation/creaming rates. Increasing the differences in density between dispersed and continuous phases also increases sedimentation/creaming rates due to increased effects of buoyancy. Creaming and sedimentation are generally considered reversible phenomena (i.e. remixing re-suspends the dispersed phase), only if the particles or droplets have not irreversibly aggregated.

1.3.2 Flocculation and aggregation

Particles and droplets in a colloidal suspension move about randomly due to Brownian motion, which leads to eventual collision between particles/droplets. According to the DLVO theory, if the sum of the attractive energies between particles is greater than the sum of repulsive energies, the particles will adhere to each other. If the attraction energy is weak, particles/droplets will be loosely held together (secondary energy minimum). This is known as flocculation and is reversible (Fig 1.3). If particles/droplets collide with enough energy to overcome the primary energy maximum, they become permanently attached to one another (primary minimum). This is known as aggregation [1].

In addition to flocculation due to random collisions, particles can also undergo bridging and depletion flocculation. Bridging flocculation occurs when the particles or droplets are stabilized by large polymers that have more than one binding site that can adsorb to particles/droplets surfaces, such as proteins. The large polymers can thus bind to one particle/droplet at one binding site and to another particle/droplet with another binding site, resulting in a bridge between the two particles/droplets [1, 10]. Bridging flocculation does not occur above a critical concentration of protein where the droplets' interfaces are fully saturated, which leaves no room for additional inter-protein binding. Depletion flocculation occurs when there are unadsorbed polymers in the continuous phase. This creates an osmotic gradient at the particles/droplets' surfaces because they are devoid of the unadsorbed polymers [1, 10]. This causes an increase in osmotic pressure in the system compared to a system containing no dispersed particles/droplets. When particles/droplets

approach each other, the volume of polymer-free solvent between them is reduced, resulting in a decrease in overall osmotic pressure. This creates a driving force for flocculation [1, 10]. Depletion flocculation does not occur at polymer concentrations that are either too low, in which case there is no appreciable increase in the osmotic pressure of the system, or too high, in which case the polymer would be present at or near enough to the droplets' surfaces, resulting in insignificant changes to osmotic pressure [1].

The rates of flocculation and aggregation are determined by the volume fraction of the dispersed phase, with lower amounts of dispersed phase resulting in less frequent collisions between particles/droplets and thus reduced flocculation/aggregation. The movement of particles/droplets due to sedimentation or creaming also increases flocculation because particles/droplets are brought into close proximity. Flocculated and aggregated particles/droplets maintain their identity as individual droplets. However, this step is a required precursor to coalescence.

1.3.3 Coalescence

Coalescence occurs when two droplets irreversibly merge into a larger daughter droplet. Stability against coalescence strongly depends on the properties of the adsorbed layer of surfactant(s) at the droplets' interface. If droplets are attracted to each other or are pushed together by an external force, a thin film of solvent forms between them. The thickness of this film depends on the balance of attractive and repulsive forces between the droplets, which is highly composition-dependent. If the adsorbed layers are charged or have hydrophilic chains extending into the continuous phase (e.g., adsorbed proteins), the film thickness is greater and contains appreciable amounts of free water. This type of film is known as a common black film (CBF) (Fig. 1.4) [5]. With proteins, the thickness of the CBF depends on pH and ionic strength. As at lower pH the proteins are closer to their isoelectric point (IEP) and there will typically be less electrostatic repulsion between the adsorbed layers. Thus, film thickness will decrease as the particles/droplets can approach each other more closely. Increasing the concentration of electrolytes also reduces film thickness as the binding of counterions to the adsorbed protein layers partially neutralizes their charge and causes a reduction in the effective ranges of their electrostatic double layers (Fig. 1.2).

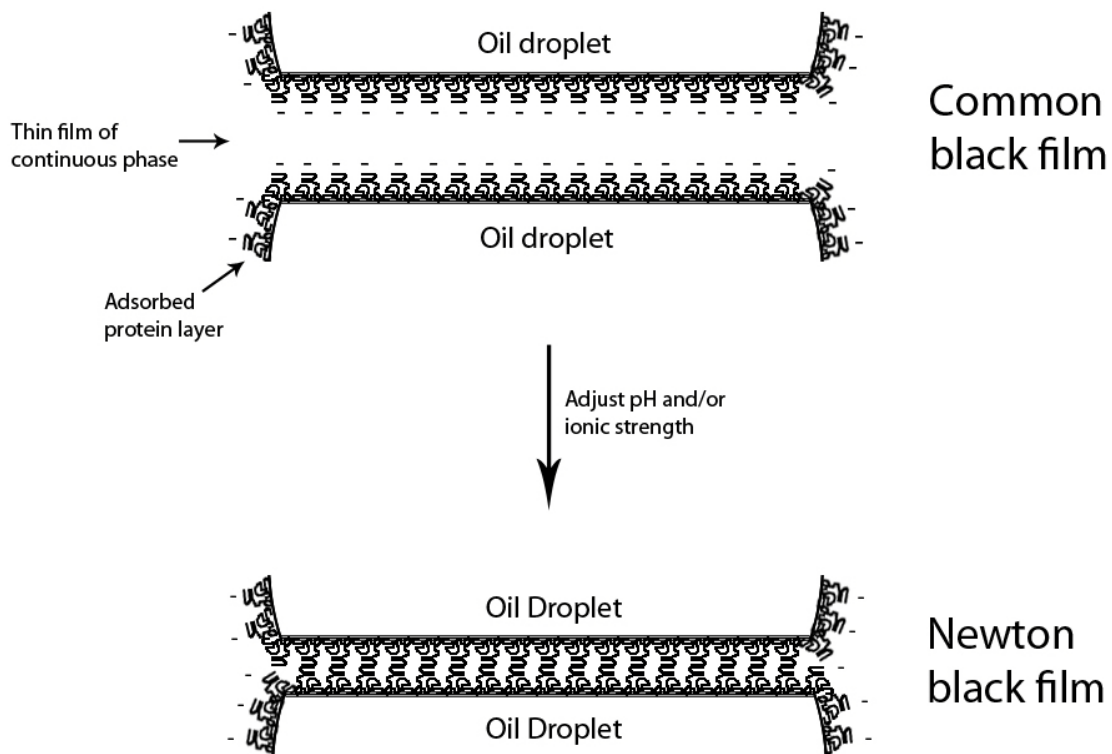


Figure 1.4 – Common and Newton black films between protein-stabilized oil droplets (adapted from [5])

If the adsorbed layers are hydrophobic, there will be very little or no free water between the droplets and the volume of the film will be very low due to hydrophobic interactions. This type of thin layer is known as a Newton black film (NBF) [5].

Coalescence occurs when the thin film separating the droplets is ruptured (Fig. 1.5). Rupturing is caused by the formation of holes in the adsorbed surfactant layers above a critical diameter. The holes may form spontaneously (spontaneous film rupture) or be caused by external forces such as pressure or shear (induced film rupture) [5]. These forces cause the adsorbed layers to thin or stretch out, resulting in a higher probability of the formation of a hole.

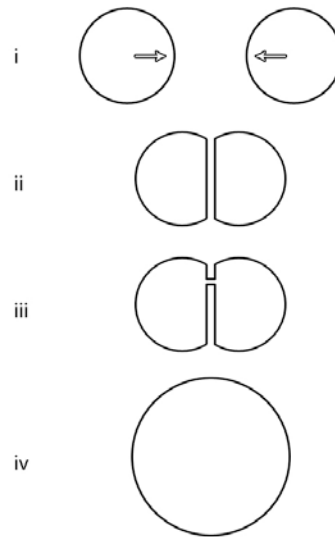


Figure 1.5 – The process of coalescence: i) two droplets approach each other, ii) a thin layer of solvent forms between the droplets, iii) rupture of the thin film due to the formation of a hole, and iv) the two droplets merge into a single larger droplet (adapted from [5]).

1.3.4 Compatibility of biopolymers

When two different biopolymer suspensions such as protein and polysaccharide suspensions are mixed, there are three possible compatibility outcomes: 1) co-solubility, 2) incompatibility, or 3) complex coacervation (Fig. 1.6), with the outcome determined by their interactions. These interactions depend on the biopolymer composition, their concentrations, pH, ionic strength, conformation, and charge density [11].

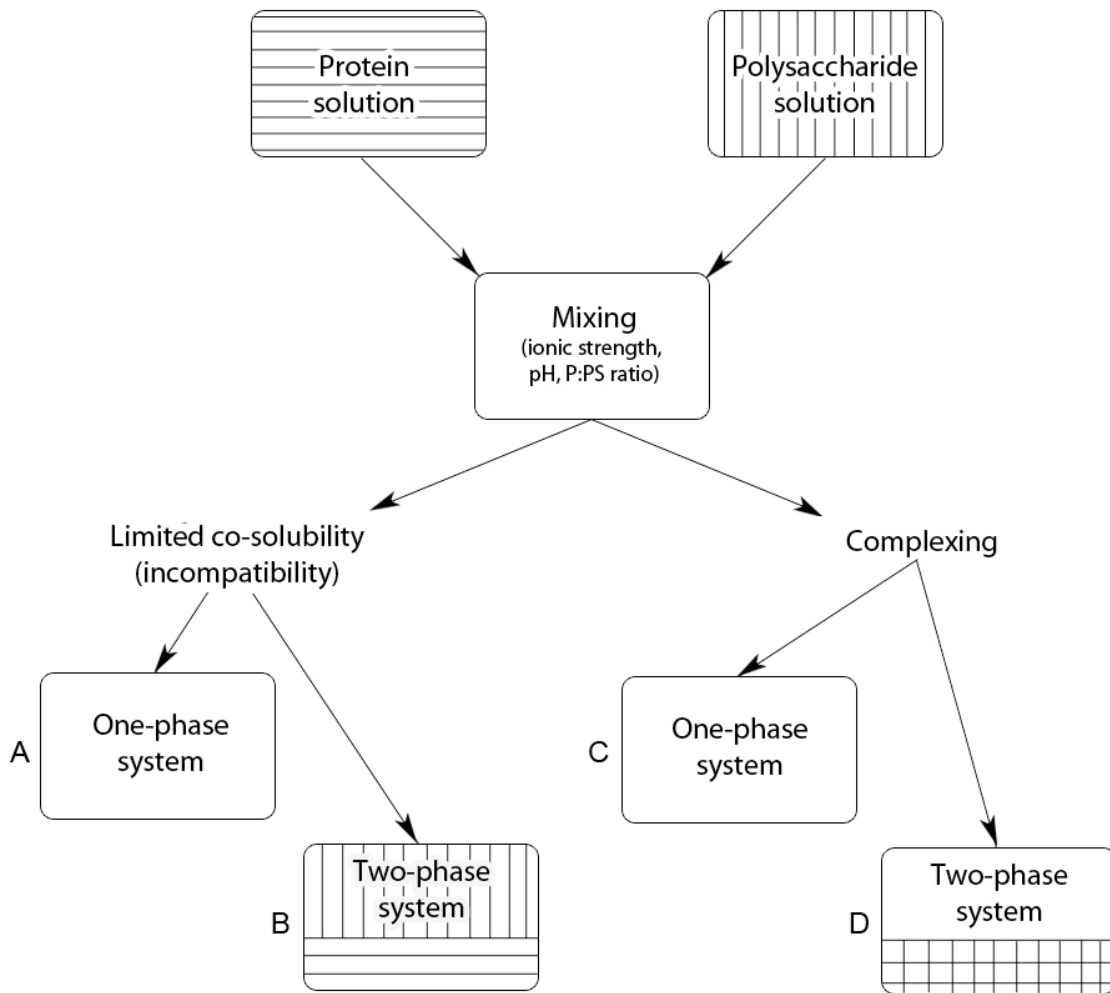


Figure 1.6 – Possible interactions between proteins and polysaccharides in aqueous suspension: co-solubility (A), phase separation (B), soluble complexes (C), and insoluble complexes (D) (adapted from [5, 10]).

Proteins and polysaccharides, below a co-solubility threshold concentration, may be miscible and exist as a homogeneous suspension (Fig. 1.6 A). Above this critical concentration, the biopolymers are incompatible, resulting in the suspension separating into two phases: one rich in protein and another rich in polysaccharide. This is known as phase separation (Fig. 1.6 B).

In aqueous suspensions, complexation between two oppositely-charged biopolymers is due to electrostatic attraction. Proteins and polysaccharides form complexes *via* electrostatic interactions at a pH that is below the IEP of the protein but above that of the polysaccharide (if charged), but only at low ionic strengths where charge screening is insignificant [12, 13]. Factors that affect compatibility and complex formation are protein/polysaccharide ratio, pH, ionic

strength, and the nature of the polymers (molecular weight, net charge, ternary structure, and flexibility of chains) [14-16]. Complex formation is usually reversible and depends on the pH and ionic strength of the suspension. At high ionic strength (0.2-0.3 M) or at pH values above the protein IEP, the complexes will dissociate. Protein-polysaccharide complexes may or may not be soluble depending on whether the adsorbed layer provides enough electrostatic or steric repulsion to prevent aggregation (Fig. 1.6 C, D) [10, 11].

1.4 Improving the stability of emulsion systems

Emulsions are inherently thermodynamically unstable due to the immiscibility of the dispersed and continuous phases. The use of emulsifiers and/or surfactants can lead to significant improvements in kinetic stability. Emulsifiers reduce the interfacial tension of droplets, allowing for the formation of smaller droplets but don't necessarily help in stabilizing the emulsion. Surfactants form an interfacial film that may have electrostatic or steric repulsion properties (such as with adsorbed proteins or surface-active polysaccharides). The adsorbed layers may also form a strong mechanical layer around the droplets which can resist coalescence. Kinetic stability may also be improved by reducing the rate of sedimentation/creaming by decreasing the size of droplets, increasing the viscosity of the continuous phase, or reducing the difference in density between the dispersed phase and the continuous phase (Eqn. 1.2) [1, 5]. Finally, reduction in dispersed phase volume fraction will minimize inter-droplet collisions and thus flocculation [1, 17].

1.5 Thesis objectives

Based on this brief survey, it is clear that the interactions between proteins and polysaccharides may be used to improve the stability of emulsions. In this regard, soy-based proteins and polysaccharides offer an ideal combination of these species, not only for their possible capacity to stabilize oil-in-water emulsions, but also as an avenue for their increased use in processed foods (discussed in chapter 2). The overall objectives of this thesis were to test for synergistic stabilizing effects between SPI and SSPS and then apply these findings to the stabilization of a model oil-in-water emulsion system. The specific objectives were:

- i) To test if SSPS was able to stabilize SPI in conditions where it would not be otherwise (low pH and high ionic strength).

- ii) To characterize the interactions between SPI and SSPS.
- iii) To explore and adapt their synergistic effects to stabilize oil-in-water emulsions.
- iv) To further elucidate the mechanism of emulsion stabilization by protein-polysaccharide interactions.

1.6 Hypotheses

The proposed hypotheses were:

- i) SSPS would be able to stabilize SPI *via* electrostatic complexation at pH values at or near the isoelectric point where SPI would normally become insoluble.
- ii) The ability for SSPS to stabilize SPI would allow for the formation of stable emulsions at acidic pH values.

1.7 Methodology and approach

SPI suspensions were shown to be stabilized by SSPS suspensions at pH values where the SPI would normally precipitate. The interactions between SPI and SSPS were characterized and the mechanisms of interaction were elucidated. These principles were then used to stabilize oil-in-water emulsions. The stability of the emulsions was then characterized over time.

Chapter 2 – Literature Review

2.0 Introduction

This chapter focuses on some of the different methods used to stabilize and characterize such emulsions with emphasis on the use of soybean biopolymers, namely SPI and SSPS.

2.1 Proteins as surfactants

Proteins are a popular choice as surfactants for food emulsions because they are naturally occurring macromolecules and thus considered ‘healthier’ than monomeric amphiphiles or low molecular weight surfactants such as polysorbates, monoacylglycerols, and lecithins [6, 11]. Proteins are amphiphilic, having both hydrophilic and hydrophobic portions, making them surface active because they are able to interact with both the oil phase and aqueous phase in an emulsion and therefore reduce the interfacial tension at droplet interfaces. In addition to emulsification activity, they can also retard droplet coalescence by forming protective layers around droplets. These layers may stabilize the droplets *via* electrostatic or steric repulsion as well as improving the mechanical strength of the interface [18].

To effectively stabilize an emulsion, proteins must ideally provide complete droplet coverage. Any exposed surfaces may lead to coalescence as the ‘bald’ areas come into contact with other droplets [6]. The efficacy of a protein’s ability to stabilize droplets may also depend on pre-treatment and processing. Exposing proteins to heating, high shear, high pressure, and treatment with extreme pH values may cause protein denaturation, which may result in the exposure of previously unexposed hydrophobic groups. Emulsification activity may be reduced if the exposure of hydrophobic groups increases inter-protein interaction or it may be improved if the newly-exposed hydrophobic groups improve binding between the protein and oil droplets [19-23]. Proteins may also be modified by various chemical treatments such as: acylation, alkylation, oxidation, phosphorylation, and deamidation, *etc.* as well as enzymatic methods such as covalent cross-linking with transglutaminase or digestion with enzymes such as proteases [24-26]. Proteins may also undergo surface denaturation after adsorption to an interface, as their conformation after adsorption changes so as to maximize the number of favorable interactions and minimize unfavorable ones (*e.g.*, contact with the oil and water phases, respectively). The rate of surface denaturation depends on the molecular flexibility of the protein with relatively flexible proteins,

such as bovine milk caseins, being able to undergo surface denaturation more rapidly than less flexible species, such as β -lactoglobulin, which are more rigid globular proteins that take longer to undergo surface denaturation. The oil phase may also affect the rate of surface denaturation, with more non-polar oils (*e.g.*, vegetable oil vs. mineral oil) causing faster surface denaturation due to hydrophobic driving forces [18]. As a result, surface denaturation may lead to the exposure of new hydrophobic or hydrophilic groups, which can result in increased attraction or repulsion, respectively, *via* hydrophobic interactions or electrostatic and/or steric repulsion [18].

Milk proteins (*e.g.*, caseins) have been the most extensively studied protein given their wide-ranging use in food applications. However, the popularity and use of soybean proteins by food processors is increasing due to the drive to find healthier, vegetable-based alternatives [2, 27, 28]. The two major components of soybean proteins are β -conglycinin (7S) and glycinin (11S) which make up 40 wt% and 30 wt% of the total seed proteins, respectively [24]. Glycinin (11S) is a hexamer with a molecular mass of 360 kDa (Fig. 2.1). It is composed at least five different subunits, with each one consisting of an acidic peptide approximately 40 kDa in weight and a basic peptide of about 20 kDa in weight linked by a disulfide bridge [29]. Its structure, solubility, and functionality change greatly with pH and ionic strength [30]. Beta-conglycinin is a trimer weighing approximately 180 kDa and consists of three different subunits (α , α' , and β , of 62, 65, and 47 kDa, respectively) [31]. Together, these proteins make up approximately 90 wt% of the total weight of SPI with the remaining 10% being composed of fat and ash [31].

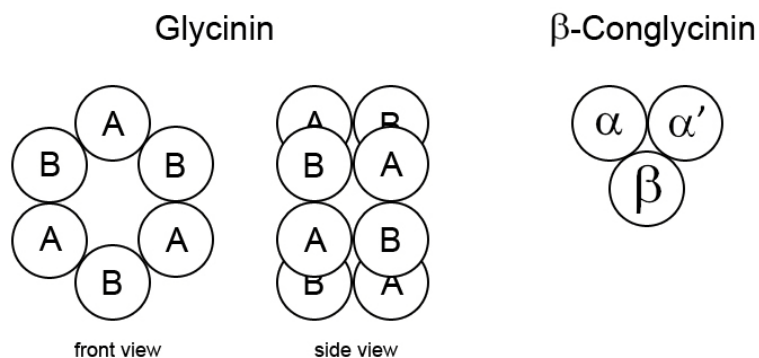


Figure 2.1 – The structure of glycinin and β -conglycinin

The structure, solubility, and functionality of SPI proteins vary with pH and ionic strength. Its solubility is at a minimum between pH 4 and pH 5 and its IEP is at pH 4.6 [22, 25, 32]. Increasing the ionic strength an aqueous suspension from 0.0 M to 0.5 M can increase solubility from near 0%

to 20%, respectively (Fig. 2.2). The addition of a salt to an aqueous protein suspension will alter the solubility of the proteins depending on the anion of the salt. The salt can either make the structure of water more organized, which results in lower protein solubility ('salting-out') due to increased hydrogen-bonding of water molecules minimizing hydrophobic contact with water, or it can break the structure of water and allow for an increase in the exposure of hydrophobic surfaces, resulting in an increase in solubility ('salting in') [33]. A recent study by Gibb and Gibb (2011) showed some evidence of salt ions binding directly to the hydrophobic surfaces of proteins, reducing the number of binding sites available for hydrophobic interactions with hydrophobic surfaces on other proteins [34]. They also found that an increase in ionic strength resulted in partial denaturation of proteins, causing them to unfold from their rigid native states into molten globule states.

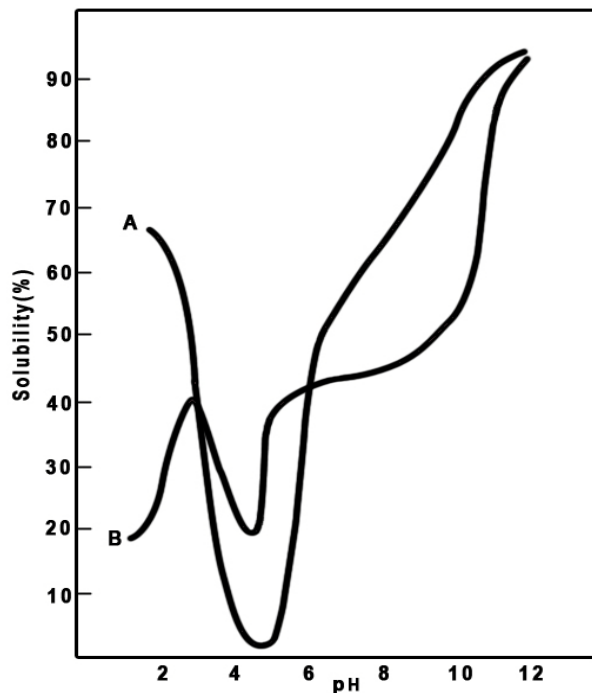


Figure 2.2 – pH-solubility profile of SPI in water in 0.0 M (A) and 0.5 M (B) ionic strength (adapted from [32]).

Increasing the ionic strength of the dispersant medium also reduces the proteins' electrokinetic mobility and zeta potential due to a reduction in the electrical double layer thickness at the protein's surface as a result of charge neutralization by counterions. The reduced range of the electrical double layer results in reduced electrostatic repulsive forces, allowing proteins to approach each other at distances close enough for attractive van der Waal forces to dominate [35]. Multivalent ions, being more charged, can penetrate further into electrical double layers and reduce

the net charge on proteins more effectively than monovalent ions. Trivalent ions penetrate further than divalent ions, which penetrate further than monovalent ions [35]. It has been demonstrated that reducing the ionic strength of glycinin suspensions has a great impact on the protein's molecular structure. At pH 7.6 and at an ionic strength of 0.5 M, glycinin is mainly present in a hexameric form (11S, 360 kDa) but when the ionic strength is lowered to 0.01 M, it dissociates into a 7S form, believed to be a trimeric form that has a more flexible, nonstructured conformation. There is no difference in solubility between the 11S and 7S forms for concentrations of up to 0.6 mg/mL [36].

SPI has been shown to have high thermal stability [37]. This is attributed to the extensive disulfide bridging within glycinin, the major protein in SPI. The denaturation temperatures of glycinin and β -conglycinin are 92 and 77°C [37], respectively. Heating glycinin breaks the disulfide bridges connecting the acidic and basic subunits and causes it to dissociate. The basic subunits then go on to self-aggregate through hydrophobic interactions to form insoluble complexes [30, 37, 38]. Heating β -conglycinin breaks disulfide bridges and causes it to dissociate into its monomers, but the monomers retain sufficient electrostatic charge to repel each other and remain fully soluble [38, 39]. The isolated proteins show different thermal denaturation behaviour compared to mixed suspensions: under conditions where glycinin would normally undergo denaturation leading to separation of its subunits that would result in aggregation, mixtures of glycinin and β -conglycinin remain stable due to β -conglycinin binding to the dissociated subunits of glycinin, thereby preventing its aggregation [37].

High pressure treatment (200 MPa) also has an effect on glycinin and β -conglycinin. In addition to causing the proteins' subunits to dissociate, it also destroys secondary protein structure by converting α -helix and β -sheet structures to random coils, though the mechanism remains to be elucidated [40, 41]. Glycinin is more susceptible to subunit dissociation than β -conglycinin and forms insoluble aggregates upon denaturation. The proteins are more susceptible to high pressure denaturation at acidic pH values due to the partial denaturation caused by their exposure to acidic conditions [41]. Tang and Ma (2009) found that high pressure treatment at 200 MPa caused increased SPI aggregation, which was unseen in untreated SPI, but aggregation decreased at higher pressures (≥ 400 MPa) due to re-solubilization of pressure-induced aggregates [42].

Glycinin and β -conglycinin have been shown to have good emulsifying abilities and are capable of stabilizing emulsions by lowering the interfacial tension between water and oil and by forming an adsorbed layer at the interface of droplets ~45 nm thick [38, 43-46]. The emulsion-

stabilizing efficacy of SPI depends on pH, ionic strength, protein concentration, and whether it has been pre-treated by heat, high pressure, or enzymatic hydrolysis. SPIs are able to effectively stabilize oil-in-water emulsions, but only at pH values sufficiently far from their IEP. Near their IEP, the proteins become insoluble and precipitate out of suspension, leading to emulsion destabilization [46]. Increased ionic strength *via* the addition of salt can lead to emulsion destabilization by two mechanisms: 1) reduction of electrostatic repulsion between droplets and/or 2) a high concentration of electrolytes, which may alter structural organization of water molecules, which in turn may alter hydrophobic interactions between non-polar surfaces [45]. In order for proteins to effectively stabilize emulsion droplets against coalescence, they must be present in sufficiently high concentration to fully cover the droplets [5]. Generally, increasing the concentration of SPI leads to more stable emulsions [47, 48]. Under controlled conditions, one can induce partial denaturation of the proteins which may lead to improved emulsifying and stabilizing capabilities [19, 38], as when they are partially denatured, they have improved freeze-thaw stability and increased tolerance to salt [19, 45]. At sub-zero temperatures, native SPI undergoes thiol/disulfide exchange reactions to form high molecular weight (from 7S and 11S to $\geq 15S$) species more susceptible to aggregation than denatured SPI [19]. Further evidence was provided by Palazolo *et al.* (2003), who found that the introduction of salt caused destabilization of native SPI-stabilized O/W emulsions but less so in thermally-denatured SPI-stabilized emulsions. They attributed this to the salt causing the formation of rigid flocs that were resistant to agitation [45]. The order of heating also has an effect on emulsion stability: heating the soy proteins before emulsification causes the formation of protein aggregates that cannot emulsify as effectively and leads to lower emulsion stability than heating after emulsification. This occurs as larger protein aggregates at droplet interfaces are more susceptible to hydrophobic interactions and flocculation [38].

Subjecting SPI proteins to high pressure treatment may improve emulsifying efficacy but not necessarily stabilizing efficacy [43]. The effect of high pressure treatment is pH dependent. Molina *et al.* (2001) found that the stability of O/W emulsions decreased with increased pressure (up to 600 MPa) at pH 7.5, with the treatment causing the dissociation of soy proteins into their subunits. Dissociated β -conglycinin subunits were soluble and had an increased emulsifying activity whereas dissociated glycinin subunits became insoluble and underwent aggregation, resulting in lower emulsion stability [43]. Similar results were reported by Puppo *et al.* (2005), who found that high pressure treatments of SPI at pH 8 resulted in better emulsifying activity but led to increased depletion flocculation in O/W emulsions. At pH 3, the SPI proteins were partially denatured due to

the acidity of the suspension which lowered the solubility of the SPI, resulting in larger droplets and increased flocculation. High pressure treatment at pH 3 improved the emulsifying ability of the acid-denatured proteins. High pressure treatment also resulted in increased adsorption of the proteins to the droplets' interfaces regardless of the pH [41]. Puppo *et al.* (2011) also showed that combined thermal and high pressure treatments resulted in significant increases in flocculation and gelation of β -conglycinin-emulsions but not for glycinin-stabilized emulsions. This was related to the difference in solubility of dissociated protein subunits [30, 37, 38]. Combined thermal and pressure treatments caused protein from the aqueous phase to adsorb and aggregate onto previously-formed protein films on the emulsion droplets' surface [21]. These surface aggregates led to increased flocculation and thus lower emulsion stability.

In addition to thermal and high pressure treatments, enzymatic treatments may also be employed to improve glycinin and β -conglycinin solubility and emulsifying properties by reducing their molecular weight thus allowing them to migrate to droplet interfaces more quickly [25, 49, 50].

2.2 Polysaccharides as emulsion stabilizers

The addition of a polysaccharide to an emulsion may have three effects. First, the polysaccharide can induce phase separation due to thermodynamic incompatibility between the polysaccharide and the emulsion droplets. This occurs *via* depletion flocculation and is dependent on the concentrations of the emulsion and the polysaccharide [51]. Second, the polysaccharide may increase the viscosity of the emulsion's continuous phase and form a gel or viscous suspension, effectively trapping droplets and retarding flocculation and coalescence. Third, the polysaccharide may interact directly with the droplet surface. As polysaccharides are normally hydrophilic, they have very low surface activity. If they are charged, they may interact electrostatically with proteins adsorbed on droplets surfaces [5]. Some polysaccharides, such as gum arabic and SSPS, contain protein moieties that increase their surface activity. The protein moieties act as anchors that bind to the hydrophobic surface of oil droplets while the carbohydrate portions of the polysaccharides stabilize the droplets *via* electrostatic or steric repulsion [52-54].

Gum arabic is a common polysaccharide used to stabilize emulsions given its high water solubility, low bulk viscosity, good emulsifying abilities, and ability to create a strong protective film around oil droplets. However, alternatives are now being sought because of variability in supply

and cost [52, 55-57]. Some alternatives to gum arabic include modified starch, pectin, and SSPS [53, 58, 59].

SSPS is a promising alternative that has been shown to have superior functional properties compared to gum arabic, modified starch, and pectin [60]. It is an acidic polymer extracted from the residual carbohydrate byproduct of SPI production, known as okara. It has a branched conformation and has a protein fraction that plays a major role in its emulsifying and emulsion-stabilizing abilities (Fig 2.3) [54].

It is an acidic polysaccharide composed of a main rhamnogalacturonan backbone branched by β -1,4-galactan and α -1,3- or α -1,5-arabinan chains, and homogalacturonan [61]. SSPS contains a hydrophilic carbohydrate portion covalently bound to a protein moiety of about 50 kDa that allows it to bind to oil-water interfaces while the carbohydrate portions form a steric barrier (~17 nm thick, though this is system-dependent) [61]. SSPS can be used to stabilize emulsions given its high water solubility (up to 30 wt%), low bulk viscosity, good emulsifying properties, and ability to form strong interfacial films [62].

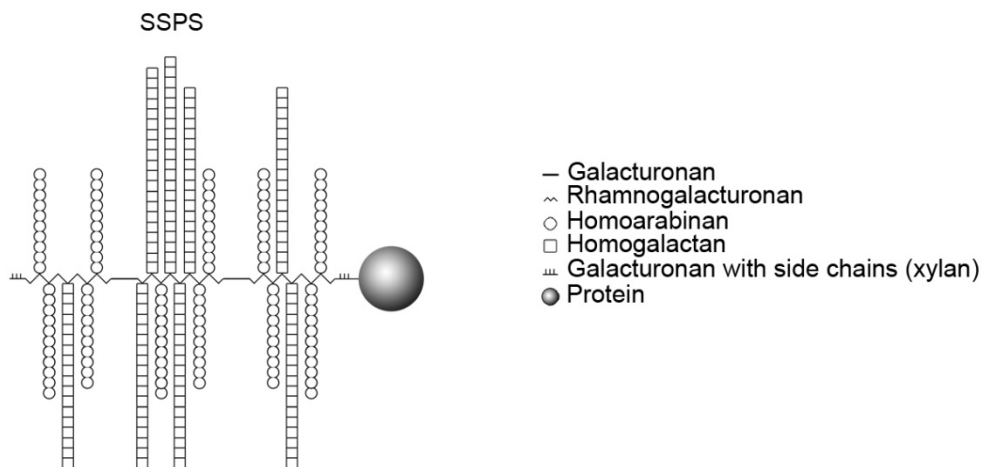


Figure 2.3 – The structure of SSPS (adapted from [63]).

The emulsifying abilities of SSPS are not affected by acidic pH or ionic strengths and it has been shown to stabilize O/W emulsions between pH 3-7 and up to 0.25 mM NaCl [60]. SSPS forms an adsorbed layer ~30 nm thick on emulsion droplets that protects them against coalescence *via* steric repulsion. The thick adsorbed layer also acts as a barrier against competitive adsorption by

small molecule surfactants, such as polysorbates, which cannot penetrate SSPS' layer of hydrophilic chains [61, 63, 64]. SSPS is also resistant to heat denaturation up to 70°C [65]. Finally, Nakamura *et al.* (2004) found that SSPS could also form complexes with milk whey protein isolate *via* electrostatic interactions, though it could also cause bridging flocculation between these species [64].

2.3 Protein-polysaccharide interactions for suspension and emulsion stabilization

There are three possible outcomes when a binary mixture of proteins and polysaccharides is prepared: 1) miscibility or co-solubility, 2) thermodynamic incompatibility, or 3) complexation (also known as coacervation) (Fig 1.6). Miscibility commonly occurs at low biopolymer concentrations. At higher concentrations, above a co-solubility threshold, thermodynamic incompatibility or complexation occurs and depends on whether the interactions are net repulsive or net attractive, respectively [66, 67]. Complexation between proteins and polysaccharides is a result of electrostatic interactions between proteins and polysaccharides when they are oppositely charged. Maximum complexation yield occurs when the proteins and polysaccharides are present at an equal ratio mixture (by weight) and at a pH where they carry an equal but opposite charge [68]. Most food proteins form complexes with anionic polysaccharides at pH values below the IEP of the protein but above that of the polysaccharide, *i.e.*, when they are oppositely charged. When proteins carry a net negative charge, protein-protein and protein-polysaccharide interactions are reduced due to electrostatic repulsion. The strength of electrostatic repulsion increases with increasing pH, where the biopolymers become more negatively charged [66]. Complexation is reversible and may be reversed by adjusting the pH or ionic strength of the continuous phase. The addition of a salt such as NaCl inhibits complexation by the binding of counterions to the polymers which neutralizes some of their charge, reduces the effective radius of their electrostatic double layers, thus resulting in charge screening. High concentrations of salt not only screen electrostatic interactions between the biopolymers but also promote their self-aggregation, which may result in destabilization of the system [11, 66, 67].

The addition of anionic polysaccharides to protein-stabilized emulsions may improve suspension and emulsion stability [14, 69-72]. Soy proteins have limited functionality at acidic pH values close to their IEP (pI 4.6), but the addition of various anionic polysaccharides (pectin,

sodium alginate, and hydroxymethylcellulose) improves their stability *via* electrostatic complexation [16, 31, 73-75]. Very little work has been done on the interaction of SPI with SSPS. Only one study, by Roudsari *et al.* (2006), has examined the effects of SSPS and high-methoxyl pectin (HMP) on SPI at low pH [76]. They found that HMP above a critical concentration of 0.05 wt% caused extensive aggregation due to depletion flocculation whereas SSPS did not for concentrations up to 0.30 wt%. They found that 0.30 wt% SSPS was the critical concentration that resulted in small droplets and monomodal droplet size distributions. HMP caused bridging flocculation at $\text{pH} \leq 4$ but emulsions containing SSPS were stable and did not show any changes in droplet size or droplet size distributions. They attributed this to the differences in the side chain compositions of pectin and SSPS: pectin contains more charged side chains than SSPS, which caused bridging flocculation between droplets. SSPS, with more neutral side chains, did not cause bridging flocculation and stabilized the droplets by steric repulsion. Roudsari *et al.* also stated that the mechanism for interaction between SPI and SSPS is still not fully understood and more work is required.

Chapter 3 – Experimental methods

3.0 Introduction

This chapter provides background information on the experimental methods used to produce and characterize the suspensions and emulsions studied. Specific parameters are discussed in chapter 4.

3.1 Protein and polysaccharide suspension preparation

Stock suspensions of SPI and SSPS were prepared by adding appropriate amounts of SPI and SSPS to give desired concentrations. These stock suspensions were then mixed together with a bench top homogenizer (Polytron PT 10-35, Kinematica GmbH, Switzerland). The Polytron PT 10-35 is a rotor-stator mixer that consists of a rotating rotor rod surrounded by a fixed stator cylinder (Fig. 3.1):

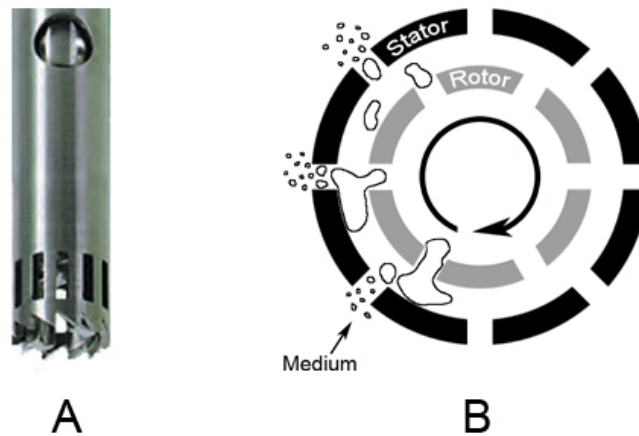


Figure 3.1 – Image of the rotor-stator of a Polytron PT 10-35 bench top homogenizer (A) and a cross-section schematic of a rotor-stator (B) (Adapted from [77]).

As the rotor spins, it forces the liquid medium into a narrow gap between the rotor and stator. The liquid is then forced through the gaps of the stator, causing shear. This shear action emulsifies the bulk liquid by breaking it down into smaller droplets [1].

3.2 Emulsion preparation

SPI and SSPS emulsions were prepared by a two-step process. First, the emulsion components were mixed with a rotor-stator to produce a coarse emulsion. The coarse emulsion was then passed through a high-pressure valve homogenizer (APV 1000, APV, Albertslund, Denmark). Fig. 3.2 depicts a schematic of how high-pressure homogenization works in an APV 1000 valve homogenizer:

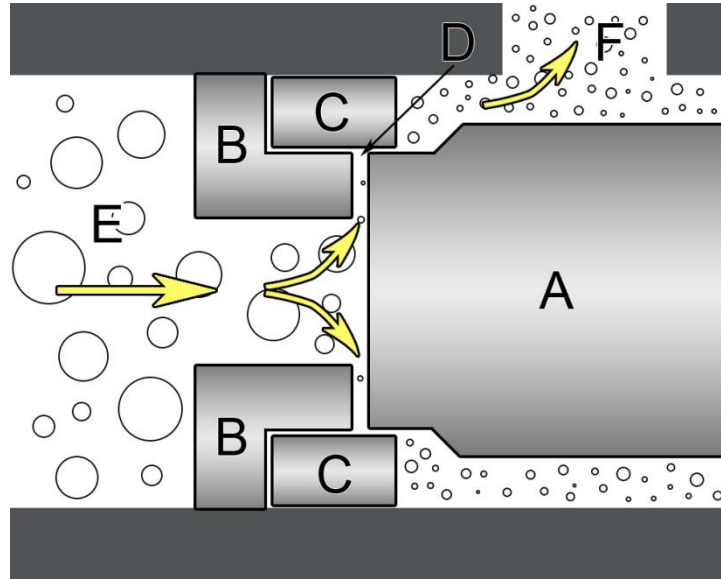


Figure 3.2 – A schematic representing the high pressure emulsification process in an APV 1000 valve homogenizer (adapted from [78]).

The coarse emulsion (E) enters the valve seat (B) at high pressure and low velocity. As the coarse emulsion flows through the small gap between the valve (A) and the seat (B), there is a rapid increase in velocity accompanied by a decrease in pressure. This produces a turbulent flow that disrupts the droplets at the discharge gap (D). The homogenized product impinges on the impact ring (C) and then flows out to be collected (F). The homogenized product can be repeatedly passed through the homogenizer to further decrease droplet size until they reach a minimum size that is governed by the pressure used [1, 10, 78].

3.3 Particle/droplet size determination

The particle or droplet sizes of suspensions and emulsions, respectively, were measured *via* integrated light scattering (Malvern Mastersizer 2000, Malvern Instruments, Worcestershire, UK). The Mastersizer 2000 has a liquid dispersion cell that pumps water through a flow cell (Fig. 3.3). As

the sample passes through the flow cell, it passes through a laser beam and causes light diffraction at angles inversely proportional to their size. The angular intensity of the scattered light is then measured by an array of photosensitive detectors. The instrument software (Mastersizer 2000 v. 5.54) then plots a map of the scattering intensity versus the scattering angle. This allows for the calculation of particle size based on the Mie theory [79]. The Mie theory solves the equation for the interaction of light with matter. It assumes that the particles are spherical and requires that optical properties such as the refractive indexes of both the particles and medium are known as well as the absorption index of the particles [80]. Integrating the scattered light at various angles around a particle allows for the calculation of its scattering cross-section which is related to its size [81]. The equation relating scattered light intensity to droplet size is:

Eqn. 3.1

where I is the intensity of the scattered light, r is the particle radius, x is the distance from the particle, λ is the wavelength of the light in the medium (equal to the vacuum wavelength λ_0 of the incident light divided by the refractive index of the dispersion medium), y is the ratio of the refractive indexes of the particle relative to the medium, and θ is the measurement angle [17].

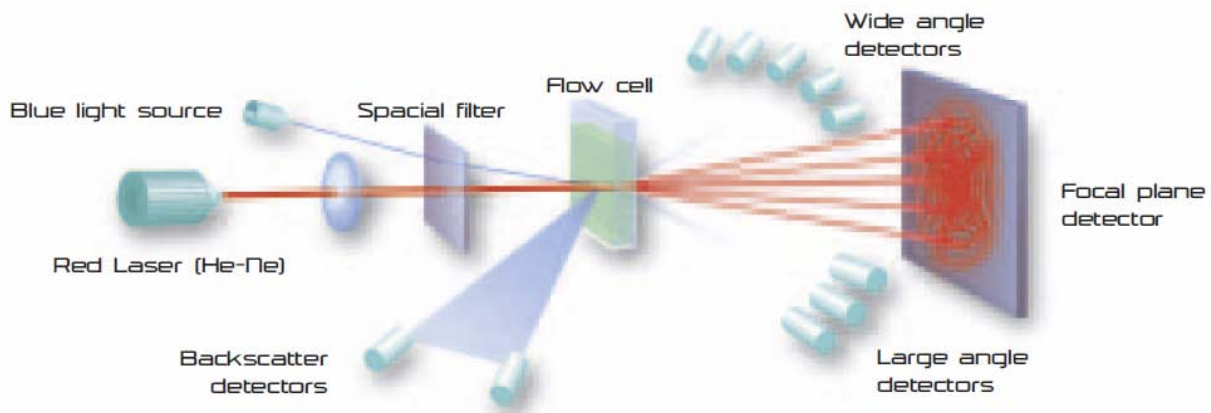


Figure 3.3 – Schematic of the Malvern Mastersizer 2000 operating principle [79].

The Mastersizer 2000 is capable of calculating the average particle or droplet size of the suspension or emulsion, respectively. Derived diameters $[D(m,n)]$ are calculated as:

Average particle or droplet sizes can be calculated as the volume-weighted mean $[D(4,3)]$ or the surface-weighted mean $[D(3,2)]$ where v_i is the number of droplets of diameter d_i [80]. In addition to calculating the average particle or droplet size of a suspension, the Mastersizer 2000 can also provide average particle or droplet size distributions by plotting the average particle/droplet size of different size bins versus their frequency count. For example, Fig. 3.4 shows a putative oil droplet size distribution from one of the many emulsions prepared during this thesis.

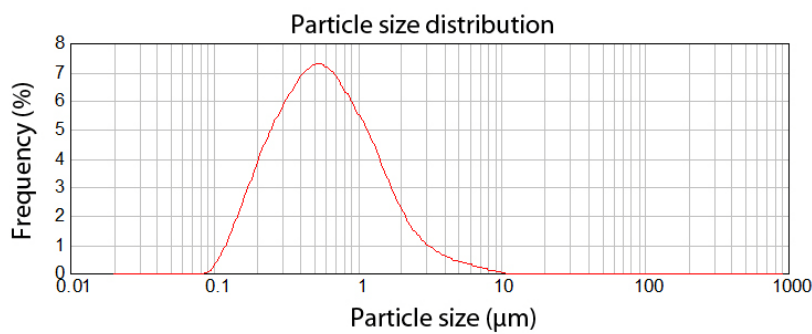


Figure 3.4 – A sample particle size distribution of an SPI-stabilized O/W emulsion at pH 8.

3.4 Surface charge determination

Particles dispersed in a liquid medium usually carry a charge represented as the electrical double layer. If an electric field is applied to the liquid medium, the particles will migrate towards either the positive or negative pole of the applied field. The direction that they travel is indicative of the charge they carry and the velocity with which they travel is proportional to the magnitude of the charge. By measuring both the direction and velocity of the particles in the presence of a known electric field, one can calculate their electrokinetic mobility and zeta potential [82].

A ZetaPlus zeta potential analyzer (Brookhaven Instruments Corporation, Holtsville, NY, USA) was used to measure the zeta potential of samples. The ZetaPlus system consists of a laser that passes through a sample that is contained within a cell that carries two electrodes that provide an electric field. The instrument measures the light scattered by the particles and compares it to a reference light beam. The frequency of the scattered light is altered due to their movement in the

electric field, a phenomenon known as Doppler shift. The frequency shift is proportional to the velocity of the particles. The instrument then uses the shift in frequency to calculate the particles' average electrophoretic mobility, μ_e :

Eqn. 3.3

For particles in a polar solvent, the zeta potential is calculated as:

Eqn. 3.4

where ζ is the zeta potential, μ_e is the electrophoretic mobility, η is the viscosity of the medium, and ϵ is the dielectric constant of the medium [82]. Zeta potential is the electrostatic potential at the surface of shear, which is the surface that separates the kinetic unit from the bulk phase (Fig. 3.5).

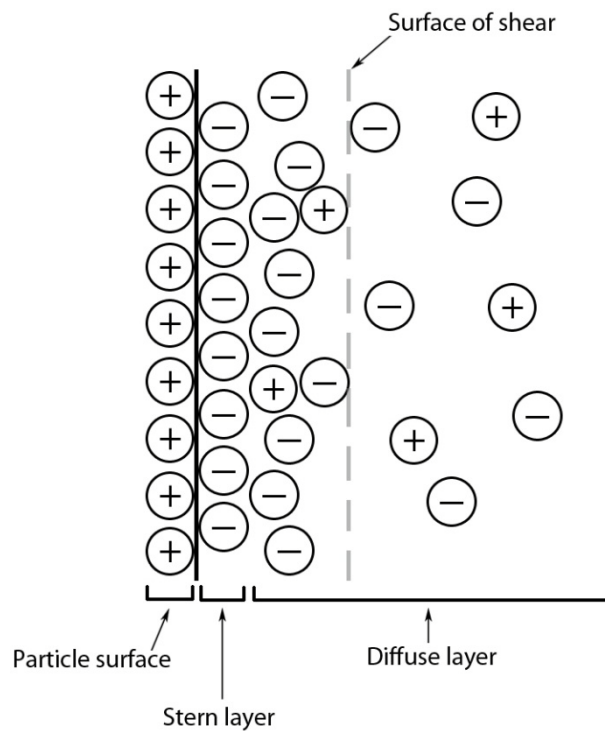


Figure 3.5 – Schematic representation of an electric double layer identifying the surface of shear (adapted from [1, 82]).

The kinetic unit consists of the charged particle, ions adsorbed on its surface (the Stern layer), counter-ions associated with it in the diffuse layer, any solvent ions that are strongly attached to the surface ions and the counter-ions. It is the kinetic unit that travels through the medium in the presence of an applied electric field. As the particle moves, it encounters friction caused by the medium. This shear force removes loosely-attached ions leaving behind the kinetic unit [82]. The exact location of the surface of shear is generally not known so the zeta potential is taken to be approximately equal to the electric potential at the Stern layer [1].

3.5 Turbidity analysis

Turbidity, also known as the apparent absorption or transmittance of light, is a measure of the total amount of light scattered as it passes through a sample [5]. The transmission of light through a sample is given by equation 3.4:

$$T_t = \frac{I_t}{I_0} = e^{-\tau x} \tag{Eqn. 3.4}$$

where T_t is the transmission, I_t and I_0 are the intensities of the transmitted and incident light, respectively, τ is the turbidity, and x is the path length through the sample [1, 10]. The intensity of scattered light depends on the particles' size and shape as well as the difference in refractive index between the particles and the medium. For dispersions, particles or droplets scatter light having an intensity I_d at a distance x from the particle according to the relationship:

$$I_d = I_0 \left(\frac{2r}{\lambda} \right)^6 \tag{Eqn. 3.5}$$

where I_0 is the intensity of the incident light beam, r is the radius of the particle, x is the distance from the particle, and λ is the wavelength of the light. Turbidity measurements can be used to estimate the average particle or droplet size of a suspension but not a distribution (Eqn. 3.5) [1].

A vertical scan turbidity analyzer (Turbiscan LAB, Formulacion, L'Union, France) was used to measure the turbidity of SPI and SSPS suspensions and emulsions. The instrument consists of a light source that sends a beam of light ($\lambda = 880$ nm) through a sample contained in a cylindrical glass vial. Two synchronous optical sensors receive light that is transmitted through and light that

is reflected the sample. One sensor is placed at an angle of 180° relative to the incident light beam and measures the transmitted light and the other is placed at an angle of 45° to the light source to measure light back-scattering intensity (Fig. 3.6).

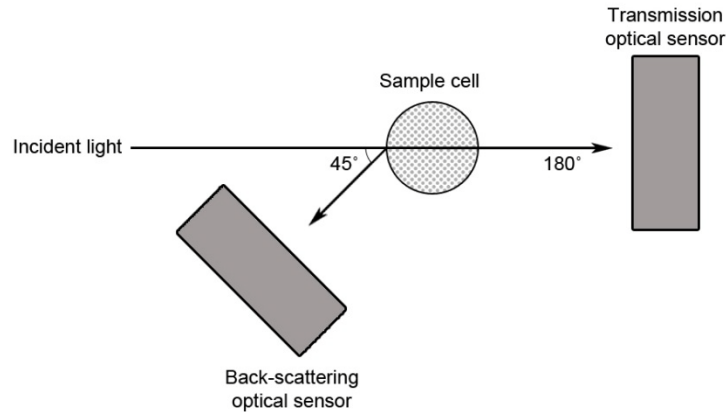


Figure 3.6 – Schematic representation of how the Turbiscan measures transmission and back-scattering (adapted from [83]).

Back-scattered light is the light reflected by the sample and is proportional to the turbidity of the sample [83]. The Turbiscan is capable of scanning the vertical length of the sample (max. 55 mm) and producing plots of sample height versus transmission and/or backscattering flux.

3.6 Light microscopy

Colloidal dispersions can be observed directly under a light microscope. A standard light microscope consists of a light source to illuminate the sample, a diaphragm to control the amount light that passes through, a stage to hold the sample slide, and a set of objectives to increase the magnification of the sample image. By using a microscope, one can examine the size and shape of particles or droplets and whether or not they are flocculated.

An inverted light microscope (Zeiss Axiovert 200M, Zeiss Canada, Toronto, ON, Canada) was used to look at SPI and SSPS suspensions and emulsions and digital images were captured with a CCD camera using software (Northern Eclipse v. 7.0, Empix Imaging, Mississauga, ON, Canada).

3.7 Data analysis

All results reported in this thesis are the arithmetic mean \pm standard deviation of triplicate experiments. Statistical analysis was performed using either a two-tailed student's *t*-test (for single pair comparisons) or one-way ANOVA with single-step Tukey's multiple comparison *post-hoc* test for multiple groups. Differences were considered statistically significant at $p \leq 0.05$.

Chapter 4 – Stabilization of oil-in-water emulsions via soy protein and soy soluble polysaccharide interactions

4.1 Introduction

This chapter summarizes the work done for the thesis, beginning with the experimental methods used to prepare and characterize the soy protein and polysaccharide suspensions and emulsions and then finishing with the results and discussion.

4.2 Materials and methods

4.2.1 Materials

A commercial SPI, PRO-FAM 974 (min. 90% protein, max. 6% moisture, max. 4% fat, and max. 5% ash), was kindly provided by Archer Daniels Midland Co., Decatur, IL, USA. A commercial SSPS, SOYAFIBE-S-CA200 (5.8% moisture, 7.8% protein, 7.8% ash, and 1.8% sodium, saccharide composition: 5% rhamnose, 3.2% fructose, 22.6% arabinose, 46.1% galactose, 1.2% glucose, and 18.2% galacturonic acid), was donated by Fuji Oil, Osaka, Japan. Soybean oil was purchased from a local grocery store and used without further purification (acid value < 0.2). HCl, NaOH, and NaCl were purchased from Fisher Scientific (Toronto, ON, Canada). Deionized water was used as the aqueous phase for the work.

4.2.2 Methods

4.2.2.1 Preparation of SPI and SSPS stock suspensions

Bulk suspensions of SPI were prepared by dissolving 2% SPI (w/w) in deionized water adjusted to pH 7 with 0.1M NaOH and 0.1M HCl. The suspension was vigorously stirred with a stir bar for three hours and then centrifuged at 7,500g for 15 minutes. The pellet was discarded and the supernatant was kept and used as a stock suspension. A stock suspension of SSPS was prepared by dissolving 1.5 wt% SSPS in deionized water at pH 7. The suspensions were vigorously stirred by magnetic stir plates for three hours to ensure complete dissolution.

4.2.2.2 Preparation of mixed SPI and SSPS suspensions

A stock suspension of 2.0 wt% SPI was mixed with a 1.5 wt% SSPS stock suspension at a 1:1 ratio and diluted with deionized water to give final concentrations of 0.75 wt% SPI and 0.75 wt% SSPS. The mixtures were then homogenized with a Polytron PT-10/35 high speed homogenizer with PCU-2 control (Kinematica GmbH, Switzerland) at 27,000 RPM for 30 seconds. The batch suspension was then divided into smaller aliquots in 50 mL falcon tubes. The pH values of the SPI and SSPS suspensions were then adjusted with 0.1M NaOH and 0.1M HCl to final pH values ranging from 3 to 8. The samples were then sealed and stored at 4°C until analysis.

4.2.2.3 Preparation of SPI-SSPS-stabilized emulsions

A primary emulsion was prepared by mixing a 1.5% SPI (w/w) suspension with soybean oil to give a 10% (w/w) oil-in-water suspension. The suspension was then homogenized with a Polytron PT-10-35 high speed homogenizer with PCU-2 control (Kinematica GmbH, Switzerland) at 27,000 RPM for 30 seconds. The coarse emulsion was then passed through a high-pressure valve homogenizer (APV 1000, Albertslund, Denmark) for 4 passes at 40 MPa. SSPS of predetermined concentrations (0%-1.5%) was then added to the primary emulsion in a 1:1 ratio to yield a final concentration of 5% oil, 0.75% SPI, and 0%-0.75% SSPS in water. The secondary emulsions were then stirred with a magnetic stir plate at 200 RPM for 60 seconds to ensure thorough mixing. The batch emulsions were then divided into smaller aliquots in 50 mL falcon tubes. The pH of the emulsions was then adjusted with 0.1M NaOH and 0.1M HCl to final pH values ranging from 3-8. The tubes were then sealed and stored at 4°C until the time of analysis (up to 28 days).

4.3 Characterization of SPI and SSPS suspensions and emulsions

4.3.1 SDS-PAGE analysis

SPI was run through a SDS-PAGE gel to characterize its components. A seven percent separating gel was prepared and loaded into a glass plate electrophoresis apparatus (Bio-Rad Laboratories, Mississauga, On, Canada). The inner chamber was filled with 1X cathode buffer and the outer chamber was filled with 1X anode buffer. 30 µL of the SPI samples and molecular weight standards were then loaded into different wells of the gel. The gel was then run for 30 minutes at 30 V and then at 125 V until the tracking dyes reached the bottom of the gel. The gels were then removed and stained with Coomassie blue R-250 staining suspension. An image of the gel was captured with a Canon SX120 IS digital camera (Canon, Toronto, ON, Canada).

4.3.2 Particle/droplet size measurement

The particle size distributions of samples were analyzed with a laser diffraction instrument (Malvern Mastersizer 2000 with a Hydro 2000S wet cell attachment, Malvern Instruments, Worcestershire, UK). Samples were gently mixed via inversion to ensure representative sampling and then dispersed in deionized water until an obscuration level of 5-10% was reached. The pH of the dispersant water was adjusted to match the pH of the samples. The background and sample integration times were 12 s and 10 s, respectively. The optical properties of the samples used were: a refractive index of 1.47 and an absorption index of 0.001 for the particles and a refractive index of 1.33 for the dispersant (water). Results were analyzed with Malvern Mastersizer 2000 software v.5.54.

Samples were analyzed after: 1, 7, 14, 21, and 28 days of storage. Values reported represent the average and standard deviation of three independent experiments.

4.3.3 Surface charge measurement

The zeta (ζ) potential of samples was measured with a Brookhaven ZetaPALS Zeta Potential Analyzer (Brookhaven Instruments Corporation, Holtsville, NY, USA). Measurements were made with a Kevlar-supported Pd electrode in a transparent 1 cm polystyrene cell. Samples were prepared by diluting 150 μ L SPI and SSPS suspension in 3.0 mL of deionized water and then mixed via inversion. The pH of the deionized water was adjusted to match that of the samples. The samples were analyzed at 25°C and the instrument settings used were: water as the dispersant with a viscosity of 0.890 cP, a refractive index of 1.330, and a dielectric constant of 78.54. Samples were measured for 5 cycles and an average value was obtained.

Samples were analyzed after: 1, 7, 14, 21, and 28 days. All experiments were performed in triplicate.

4.3.4 Turbidity and sedimentation/creaming

All dispersions were optically characterized using a vertical scan analyzer (Turbiscan LAB, Formulation, L'Union, France). The turbidity of samples was characterized by measuring the transmission and backscattering of incident light ($\lambda = 880 \text{ nm}$) along the height of an optical glass tube by two synchronous detectors. The transmission detector was set at an angle of 180° and the backscattering detector was set at an angle of 45° . Samples were prepared by filling glass vials (20 mm diameter) up to a 40 mm mark and then sealing with a cap. The entire length of the sample was scanned and the turbidity profiles were analyzed with Turbiscan LAB Turbisoft LAB EXPERT software v 1.14.0. All samples were analyzed at 25°C .

Samples were analyzed after: 1, 7, 14, 21, and 28 days of storage. Experiments were performed in triplicate.

4.3.5 Inverted light microscopy

A Zeiss Axiovert 200M inverted light microscope (Zeiss Canada, Toronto, ON, Canada) with a 10X objective and 1X ocular lens was used to examine samples at 25°C . Images were captured with a CCD camera and analyzed with Northern Eclipse software, v.7.0 (Empix Imaging, Inc., Mississauga, ON, Canada).

4.4 Results and Discussion

4.4.1 Characterization of SPI and SSPS suspensions

4.4.1.1 SDS-PAGE analysis

SDS-PAGE analysis of the SPI showed that all of the subunits of both glycinin (7S α , α' , and β) and β -conglycinin (11S A and B) were present, indicating that the commercial SPI contained both proteins (Fig. 4.1) [31, 38, 84]. During the protein extraction and purification process, proteins may undergo denaturation and hydrolysis if treated with harsh conditions such as high heating temperatures, high ionic strengths, or extreme alkalinity or acidity. This would result in a change in the molecular weight profiles of the proteins, leading to unexpected bands due to protein aggregates (higher molecular weights) or protein hydrolysis (lower molecular weight). This may be the cause of the faint bands seen at 116, 60, and 16 kDa.

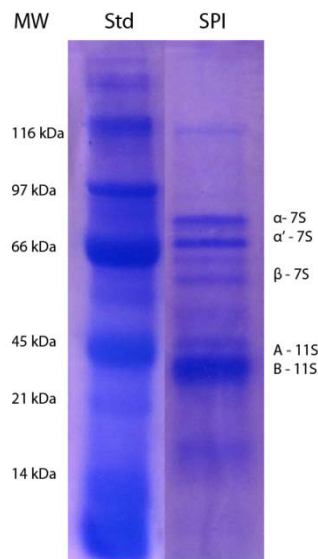


Figure 4.1 – SDS-PAGE gel of molecular weight standards (Std) and SPI.

4.4.1.2 Particle size distributions

The stability of SPI was affected by both pH and concentration of SSPS (Fig. 4.2). These effects were strongly related to the pH-dependence of SPI's solubility. Glycinin and β -conglycinin both have an isoelectric point (IEP) of 4.6, where their overall net charge is zero and solubility is at a minimum [22, 35].

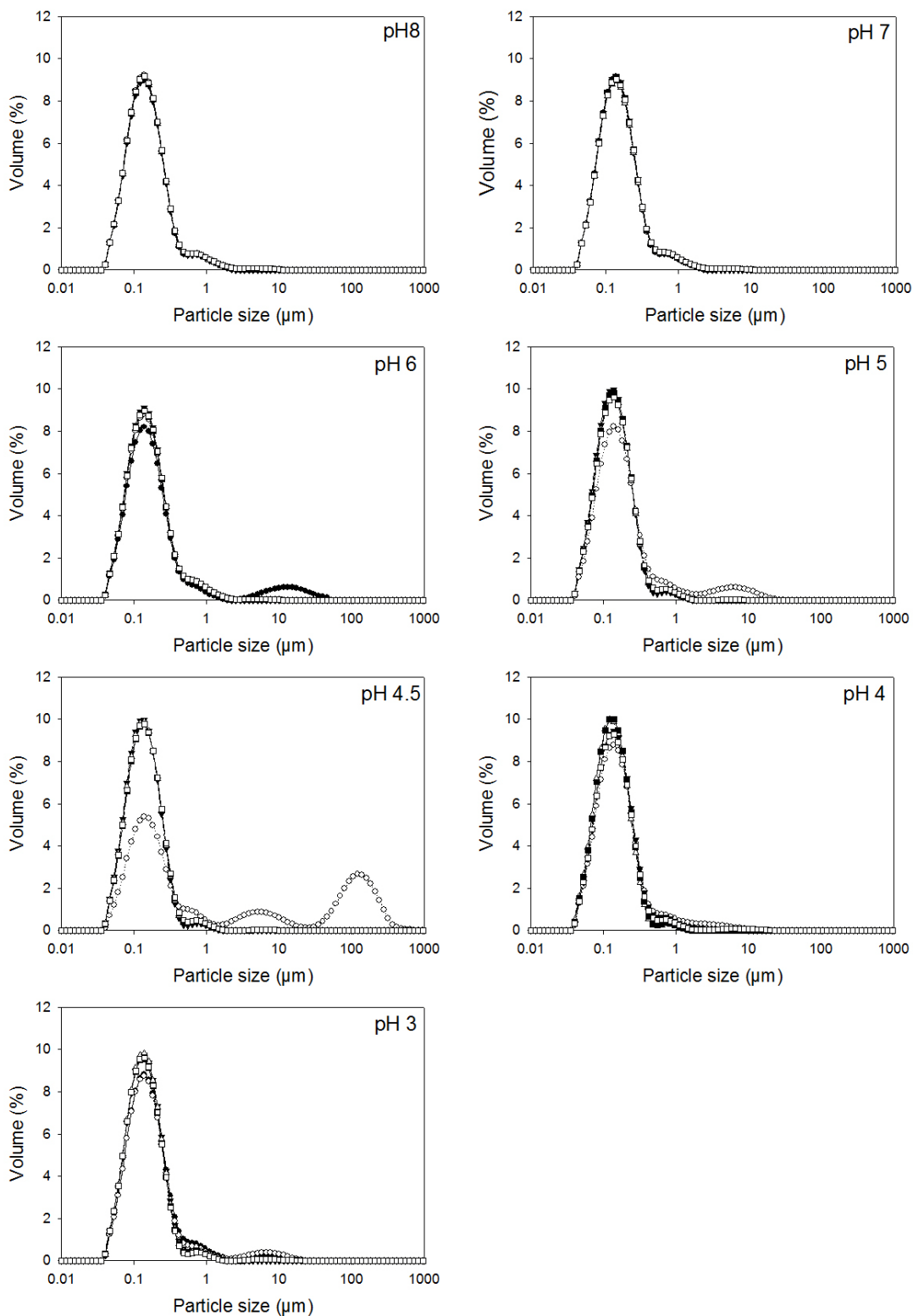


Figure 4.2 – The effect of pH on the particle size distributions of 0.75 wt% (w/w) SPI suspensions with varying amounts of SSPS after 24 h of storage: 0 wt% (●), 0.05 wt% (○), 0.125 wt% (▼), 0.25 wt% (△), 0.375 wt% (■), and 0.50 wt% (□) (n=3).

At pH 8 and 7, the proteins' solubility is at a maximum at ~80 wt% [32]. At pH 6, their solubility decreases to about 35 wt% (Fig. 2.1) [22, 32]. This is due to a decrease in the net charge of the proteins, leading to a reduction in the electrostatic repulsive forces between particles [10]. Aggregation occurs if electrostatic repulsive forces are weaker than attractive hydrophobic forces. This behaviour was observed at pH 6 for control suspensions where the lack of SSPS to stabilize the proteins led to aggregation, evidenced by an increase in larger particles ca. 10 μm . At pH 5, 4.5, and 4, near the IEP of SPI, the proteins were at their solubility minimum and precipitated from suspension and thus no particle size distributions (PSDs) were available. At pH 3, below their IEP, the proteins had an overall positive charge (Fig. 4.3) that caused electrostatic repulsion between particles which increased their solubility and stability. The particle size distribution of the control suspension at pH 3 showed a slight increase in particle size compared to pH 7 and 8, which was probably due to the pH of the suspensions not being adjusted quickly enough during sample preparation, thus allowing for some protein aggregation.

Above a critical concentration (0.25 wt%), the presence of SSPS increased the stability of the SPI against aggregation and phase separation. Below this concentration, SSPS presumably did not sufficiently cover the surface of the SPI protein, resulting in aggregation, possibly due to bridging flocculation. Nakamura *et al.* (2004) found that SSPS was capable of causing bridging flocculation in milk-whey-protein-stabilized O/W emulsions which resulted in phase separation [64]. At pH 8 and 7, both SPI and SSPS are negatively-charged, resulting in electrostatic repulsion between the biopolymers that led to co-solubility (Fig. 1.6). The net charge of SPI became more positive as pH decreased, allowing for electrostatic interactions with the negatively-charged SSPS. Roudsari *et al.* (2006) postulated that once bound to SPI, SSPS provided stabilization via electrostatic and steric repulsion [76]. From the zeta potential data of the SPI-SSPS suspensions (Fig. 4.3), it was observed that the addition of SSPS to SPI suspensions caused charge neutralization, suggesting that there was complexation. The SPI-SSPS complexes did not exhibit aggregation even though the overall net charge was zero (zeta potential of ~ 0 mV), suggesting that SSPS stabilized SPI via steric repulsion rather than electrostatic repulsion. Steric stabilization by SSPS has been attributed to the highly branched structure of its large neutral chains [76]. There was no increase in particle size with the addition of higher concentrations of SSPS at any pH, suggesting that SSPS did not cause bridging or depletion flocculation at these concentrations.

4.4.1.3 Surface charge

Surface charge measurements showed a trend of increasing zeta potential with decreasing pH. This was expected as at higher pH values SPI was more negatively charged. The net charge of SPI decreased with decreased pH and resulted in increased zeta potential. Correlating with the PSD data above, above a critical concentration of 0.25 wt%, SSPS was able to stabilize 0.75 wt% SPI over the entire range of acidic pH values studied. At pH 8 and 7, there was little interaction between the SPI and SSPS due to like negative charges which led to a zeta potential maximum of ca. -40 mV. As the pH decreased, the proteins became more positively charged, resulting in increased zeta potential. At pH 5, 4.5, and 4, near SPI's IEP, the net charge of the proteins was neutral which led to a zeta potential of zero (note: the zeta potential measurements were unavailable for these points due to precipitation of the protein and these values were based on findings by Chen and Soucie [35]). Suspensions containing SSPS remained negatively-charged due to SSPS binding positive patches of protein which left the complexes with an overall negative charge. Chen and Soucie (1986) postulated that a decrease in electrophoretic mobility, i.e. a decrease in zeta potential, was due to electrostatic binding between oppositely-charged molecules or ions [35]. This was especially evident at pH 3, where the zeta potential decreased with increasing concentrations of SSPS up to a critical concentration of 0.25 wt%, where it was presumed that the protein surfaces became saturated with SSPS and thus no significant decreases in zeta potential were seen for 0.50 and 0.75 wt% SSPS ($p \leq 0.05$).

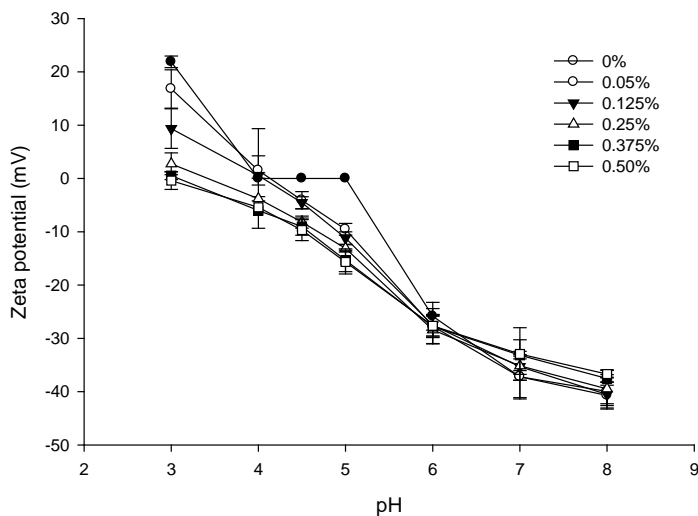


Figure 4.3 – The effect of pH on the zeta potential of 0.75 wt% SPI suspensions with varying concentrations of SSPS after 24 h of storage: 0 wt% (●), 0.05 wt% (○), 0.125 wt% (▼), 0.25 wt% (△), 0.375 wt% (■), and 0.50 wt% (□) (n=3).

Bengoechea *et al.* (2011) studied the complexation of lactoferrin with pectin and found that the zeta potential of protein suspensions became more negative with the addition of polysaccharide and attributed it to complexation between the protein and polysaccharide [85]. This trend continued until a saturation concentration was reached where the zeta potential of the suspensions plateaued and did not decrease with further addition of polysaccharide.

Generally, zeta potential values of ≤ -30 mV or $\geq +30$ mV are required for particles to be considered stable against aggregation due to electrostatic repulsion [86]. Although the zeta potential for the SPI-SSPS suspensions were lower than ± 30 mV below pH 5, the suspensions remained stable and showed no signs of phase separation for the 7 days that they were studied (data not shown). This suggested that SSPS stabilized SPI *via* steric repulsion rather than electrostatic repulsion [54].

4.4.1.4 Turbidity and sedimentation

The sedimentation of 0.75 wt% SPI suspensions was affected by pH and the presence of SSPS (Fig. 4.4). Control suspensions underwent sedimentation near SPI's IEP whereas SPI suspensions containing at least 0.25 wt% SSPS did not, which indicated the stabilizing effect of the SSPS. The phase behaviour of mixed protein and polysaccharide suspensions depends on the pH, ionic strength, and concentrations [5, 10, 11]. Below critical concentrations, the biopolymers may be co-soluble and exist as a monophasic suspension. Above these threshold concentrations, the biopolymers may undergo phase separation. The addition of higher concentrations of SSPS did not cause phase separation of the suspensions, suggesting that SSPS did not cause bridging or depletion flocculation up to concentrations of 0.75 wt% [10].

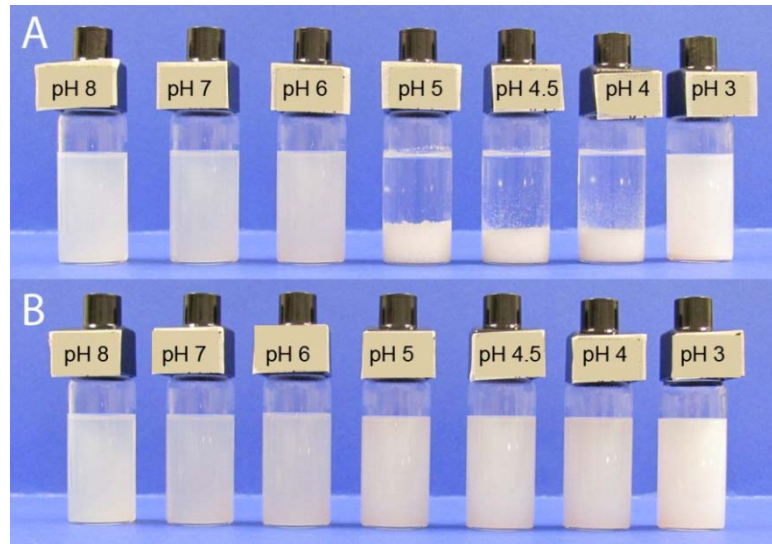


Figure 4.4 – The effect of pH on the sedimentation of 0.75 wt% SPI control suspensions (A) and 0.75 wt% SPI + 0.25 wt% SSPS suspensions (B) after 24 h of storage.

The sample height-dependent turbidity profiles of control suspensions are shown below (Fig. 4.5). Light transmission through the samples was uniform throughout the entire height of the sample at pH values where the protein is sufficiently charged for electrostatic repulsion (pH 8, 7, 6, and 3). At pH values near the IEP (pH 5, 4.5, and 4), the particles aggregated and sedimented. This resulted in a serum supernatant devoid of particles, which resulted in high light transmission. The thickness of the sediment and serum layers were used to calculate the sedimentation rates of the samples over time. Suspensions containing SSPS showed uniform transmission profiles, demonstrating a lack of sedimentation. This meant that SSPS was able to stabilize SPI over the entire pH range tested.

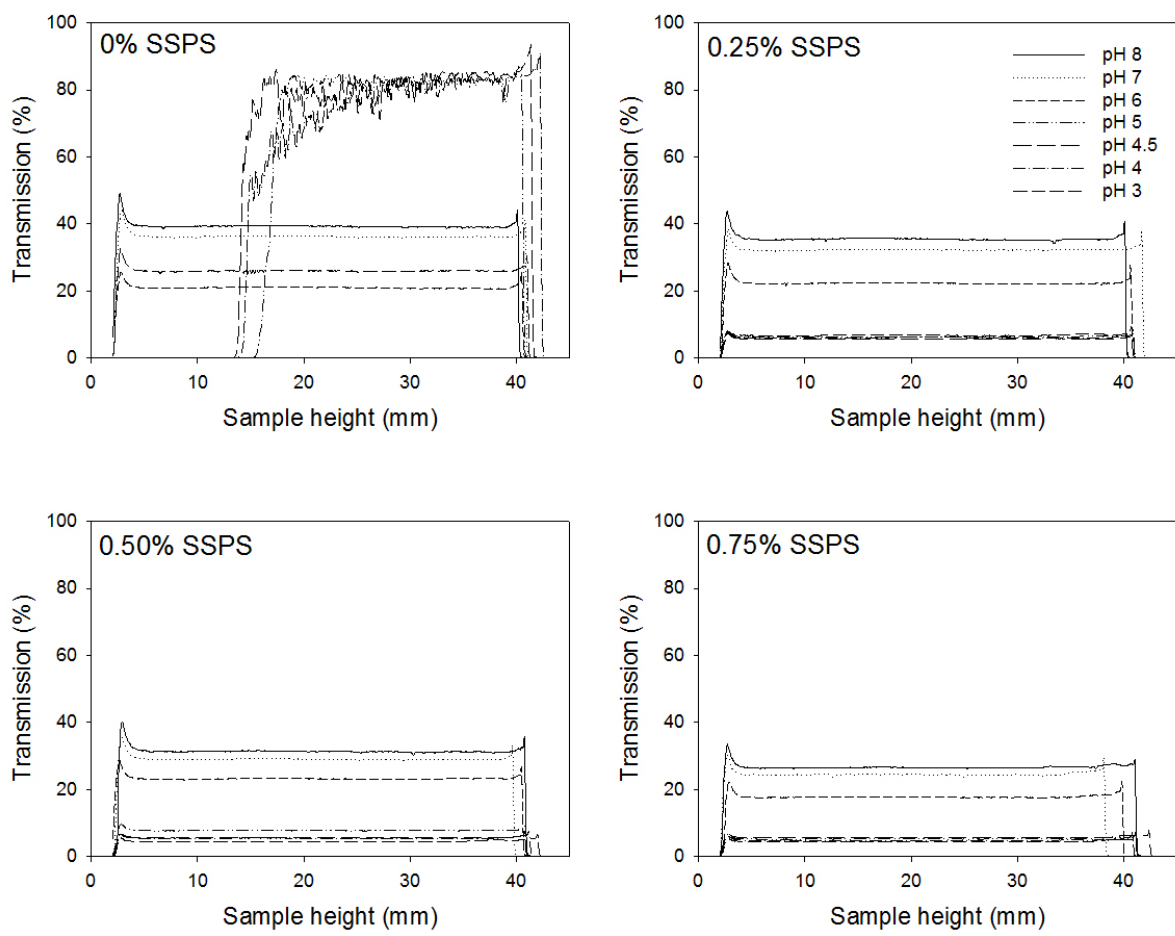


Figure 4.5 – The effect of pH on transmission profiles of 0.75 wt% SPI suspensions with varying concentrations of SSPS.

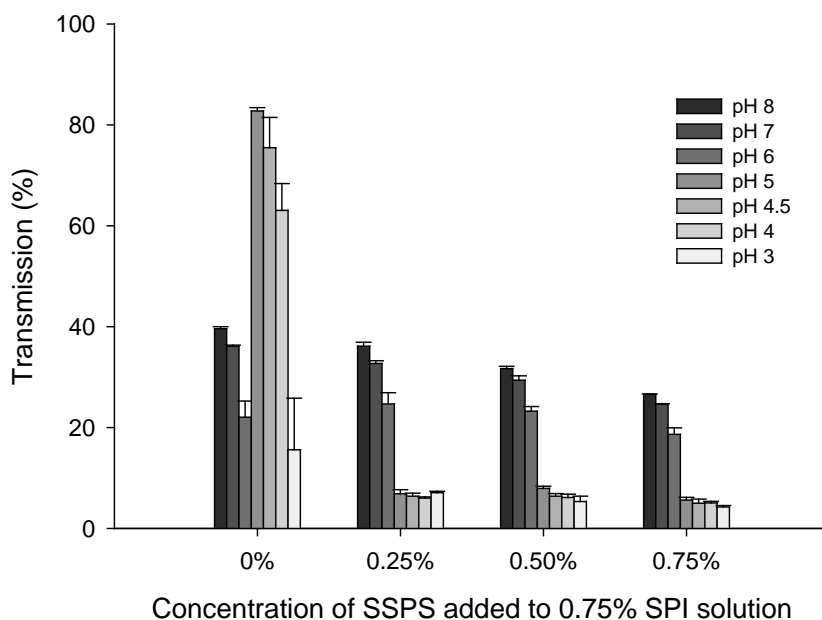


Figure 4.6 – The effect of pH on the transmission of 0.75 wt% SPI emulsions with varying concentrations of SSPS (n=3).

Suspension turbidity increased with decreasing pH (Fig. 4.6).. The high transmission values, *i.e.* low turbidity, of control suspensions compared to suspensions containing SSPS at pH 5, 4.5, and 4 , were due to isoelectric precipitation of SPI which caused the protein aggregates to sediment to the bottom of the samples resulting in a particle-depleted serum layer on top (Fig. 4.4). Addition of SSPS stabilized the SPI suspensions but showed a trend of increasing turbidity with decreasing pH. This was presumably caused by the complexation of SPI and SSPS which resulted in larger particles which absorbed more light (Eqn. 3.5). At pH 8 and 7 there was no interaction between SPI and SSPS due to electrostatic repulsion (both SPI and SSPS were negatively charged) and thus smaller particle sizes. SPI-SSPS complexation increased with decreasing pH, which would result in larger particle sizes and higher turbidity. In the pH range 3-5 there were no significant differences in transmission between SSPS-stabilized suspensions ($p \leq 0.05$) possibly because the binding of SSPS to SPI did not result in significant differences in particle sizes at these pH values (Fig. 4.2).

Another trend observed was that transmission decreased with increasing amounts of polysaccharide in suspension. This was attributed to the increase in particle concentration in the samples, which is related to the amount of transmitted light by the Beer-Lambert law:

$$T = 10^{-\epsilon \ell c}$$

Eqn. 4.1

where T is transmission, ϵ is molar scattering capacity, ℓ is path length of the sample, and c is sample concentration. The transmission values observed were lower than those predicted by the additivity properties of turbidity, i.e., the turbidity of SPI+SSPS suspensions were more turbid than predicted. Giancone *et al.* found similar trends for mixtures of pectin and soy flour, where it was found that the mixed suspensions had higher turbidity than pure suspensions. They attributed the decrease in transmission to complex formation between the pectin and soy flour which led to increased particle size and thus higher turbidity [74].

The suspension sedimentation rates were studied over 28 days. Sedimentation was defined as the percent of suspension layer ($F_{\text{suspension}}$) retained over time:

$$\text{Eqn. 4.2}$$

where $h_{\text{suspension}}$ and h_{total} are the height of the suspension layer and total height of the sample, respectively. Only the control samples (0% SSPS) exhibited sedimentation, which was highest at the IEP of SPI (pH 5, 4.5, 4) (Fig 4.7). Sedimentation was also observed for suspensions at pH 3, but at lower values than suspensions at pH 5, 4.5, and 4. Sedimentation was caused by charge neutralization which led to protein precipitation. There was no significant difference in the amount of sedimentation between samples at pH 5, 4.5, and 4 ($p \leq 0.05$) and sedimentation rates did not change over 28 days ($p \leq 0.05$).

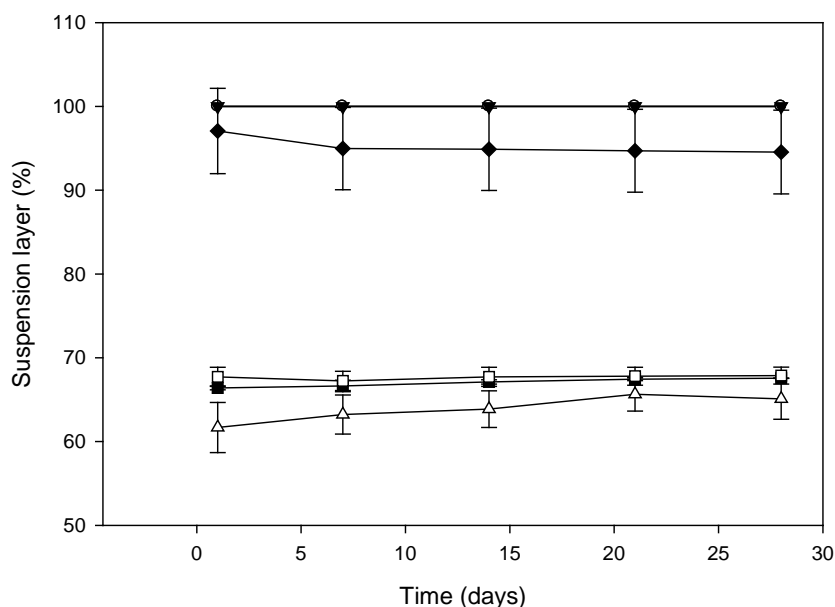


Figure 4.7 – Sedimentation of 0.75 wt% SPI control suspensions over time at pH 8 (●), pH 7 (○), pH 6 (▼), pH 5 (△), pH 4.5 (■), pH 4 (□), and pH 3 (◆).

4.4.1.5 Effect of ionic strength

It was hypothesized that the SSPS underwent complexation with the SPI proteins via electrostatic interactions at pHs below or near SPI's IEP, where the proteins would carry overall positive charges or contain positive patches, respectively, and above the IEP of SSPS ($\sim pI$ 3 [10]) where the polysaccharide would be negatively-charged. To test this hypothesis, the ionic strength of the suspensions was increased by adding 1 wt% (w/w) NaCl to suspensions containing 0.75 wt% SPI with 0.75 wt% SSPS which were previously shown to be stable over the pH range studied (pH 3-8) (Fig. 4.4). It is known that increases in ionic strength can disrupt electrostatic interactions between proteins and polysaccharides via charge screening by electrolytes as well as by promoting self-association of molecules [67, 87].

As shown below, the addition of salt caused destabilization of the SPI-SSPS suspensions (Fig. 4.8).

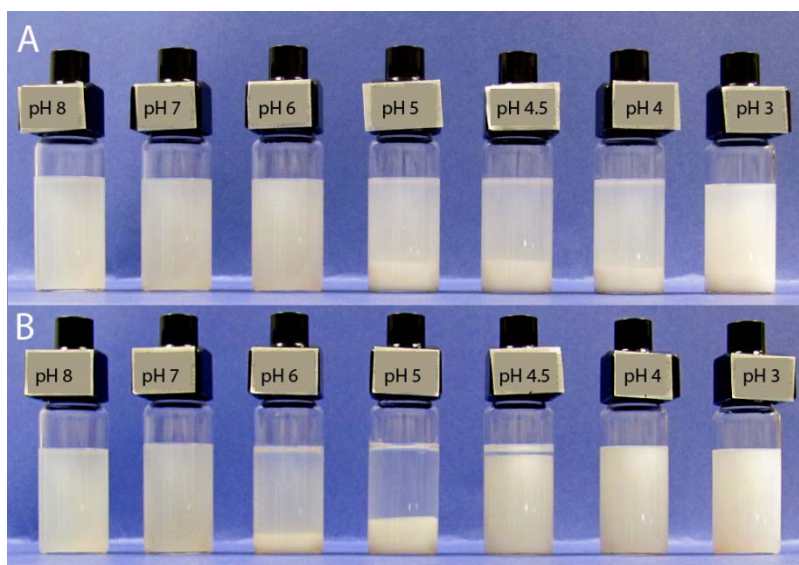


Figure 4.8 – Sedimentation of 0.75 wt% SPI + 0.75 wt% SSPS suspensions after 24 h of storage with 1 wt% NaCl added before SPI/SSPS mixing and pH adjustment (A) and 1 wt% NaCl added after mixing and pH adjustment (B).

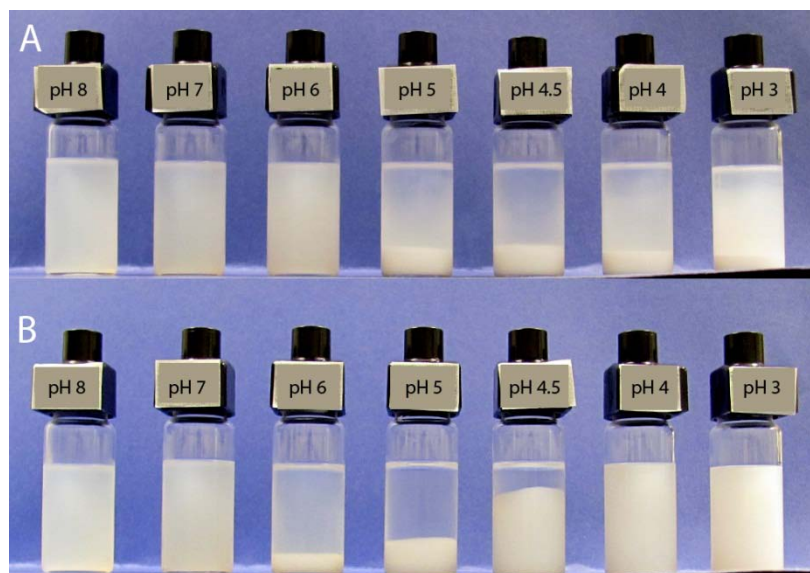


Figure 4.9 – Sedimentation of 0.75 wt% SPI + 0.75 wt% SSPS suspensions after 14 days of storage with 1 wt% NaCl added before SPI/SSPS mixing and pH adjustment (A) and 1 wt% NaCl added after mixing and pH adjustment (B).

At pH 8 and 7, there was no difference in sedimentation behaviour for suspensions with salt added before (Fig. 4.8 A) or after (Fig. 4.8 B) mixing and pH adjustment, suggesting that 1 wt% NaCl was not enough to cause a significant reduction in the particles' electrostatic double layers and they were able to maintain electrostatic repulsion between particles. As the pH decreased, there was a marked difference between the two treatments, indicating that the order of addition of salt had a significant effect on sedimentation behaviour. At pH 6, the addition of salt before mixing and pH adjustment did not cause sedimentation whereas it did when the salt was added afterwards. This may have been due to the Na⁺ and Cl⁻ ions electrostatically screening the SPI and SSPS particles, which would have prevented them from forming complexes and so they remained co-soluble. The sedimentation that resulted from the addition of salt after mixing and pH adjustment was likely due to formation of SPI-SSPS aggregation. At pH 6, SSPS may bind to positive patches on the SPI particles, forming complexes. The addition of salt may have caused electrostatic screening of some of the patches which allowed for interaction and aggregation between complexes (Fig. 4.10). As the pH was further decreased, sedimentation was observed for both treatments, although there was a difference in trends. For the suspensions with salt added before mixing and pH adjustment, sedimentation was observed for all samples at pH ≤5 and there was no significant difference in the amount of sedimentation ($p < 0.05$). SPI+SSPS suspensions with salt added after mixing and pH adjustment showed sedimentation at pH 5 and 4.5, but not at pH 4 and 3. Sedimentation decreased with decreased pH. Similarly to what might be happening at pH 6, this may be due to aggregation of SPI-SSPS complexes. The differences in turbidity between the two treatments also support this theory since the samples with salt added before mixing and pH adjustment remain more turbid than samples with salt added after, indicating that some SPI was left in the suspension layer of samples with salt added before compared to samples with salt added after. The suspension layer of samples with salt added after was less opaque, probably due to SPI forming complexes with SSPS and then precipitating out upon the addition of salt. Samples at pH 4.5 showed less sedimentation than samples at pH 5 and 6 and no sedimentation was observed for samples at pH 4 and 3. The decrease in sedimentation with decreased pH may be due to increased interactions between the SPI and SSPS, which resulted in impermeable barriers against salt penetration and prevented disruption of their electrostatic bonds [1]. Overall, the order of the addition of salt had a significant effect on the stability of the SPI+SSPS suspensions. If the salt was added before mixing and pH adjustment, destabilization occurred because the salt could effectively screen the SPI and SSPS which prevented complexes from forming while promoting self-association of the biopolymers which caused aggregation and precipitation. The addition of salt after the formation of SPI-SSPS

complexes had a different effect as the salt had to penetrate into the complexes before it could cause electrostatic screening. There were no significant changes in sedimentation and trend for all samples except for the sample with salt added after at pH 4.5, which exhibited increased sedimentation after 14 days (Fig 4.9).

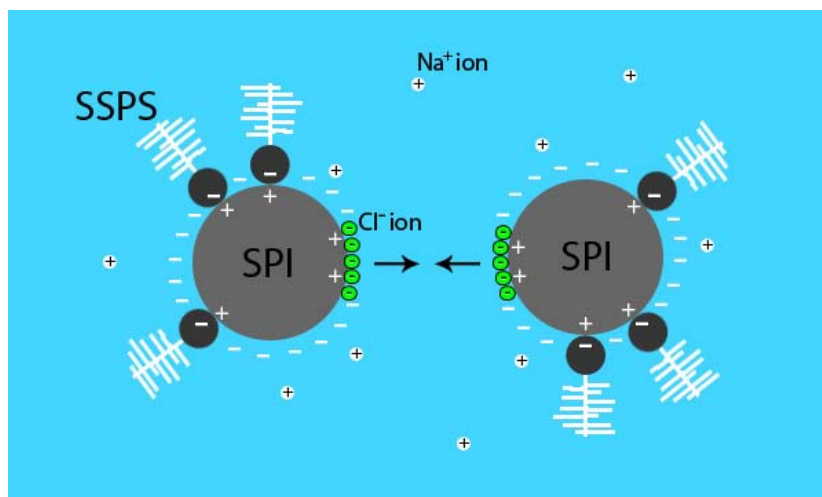


Figure 4.10 – The possible effect of NaCl on interactions between SPI-SSPS complexes

The addition of salt also caused changes in the particle size distributions of samples and resulted in shifts to larger particle sizes compared to control suspensions (Fig. 4.11). The data are in agreement with the sedimentation behaviours seen above - for samples with salt added before mixing and pH, smaller particle sizes were seen at pH 8, 7, and 6, correlating with the lack of sedimentation (the small particles were soluble in suspension). At $\text{pH} \leq 5$, larger particles were observed and were the cause of sedimentation. The particle size data for samples with salt added after mixing and pH adjustment also followed the sedimentation trends observed above - particle sizes were smallest at pH 8, 7, 4, and 3, where no sedimentation was observed. Samples at pH 6, 5, and 4.5 had larger particle sizes, which caused sedimentation.

Suspension pH as well as the presence of salt and its order of addition had significant effects on suspension particle size distribution (Fig. 4.10). At pH 8 and 7, the increase in ionic strength caused a decrease in the population of smaller particles and an increase in larger ones, indicating aggregation. This was due to the sodium chloride ions acting as counterions which reduced the effective radii of the electric double layers of the particles causing electrical double layer compression, but only enough to cause loosely-flocculated aggregates since no sedimentation was

observed and no aggregates were seen under the microscope (Fig. 4.13). At pH 6, the addition of salt after mixing and pH adjustment caused a shift to large particle sizes, which was the cause of sedimentation seen earlier, whereas adding salt after only caused a slight increase in aggregation. There was no difference in suspension particle size distributions between treatments at pH 5. However, at pH 4.5, 4, and 3, the addition of salt after mixing and pH adjustment resulted less flocculation, evidenced by the smaller population of larger particles. The PSDs of samples with salt added before mixing were not affected by pH. These data correlate with the sedimentation data above.

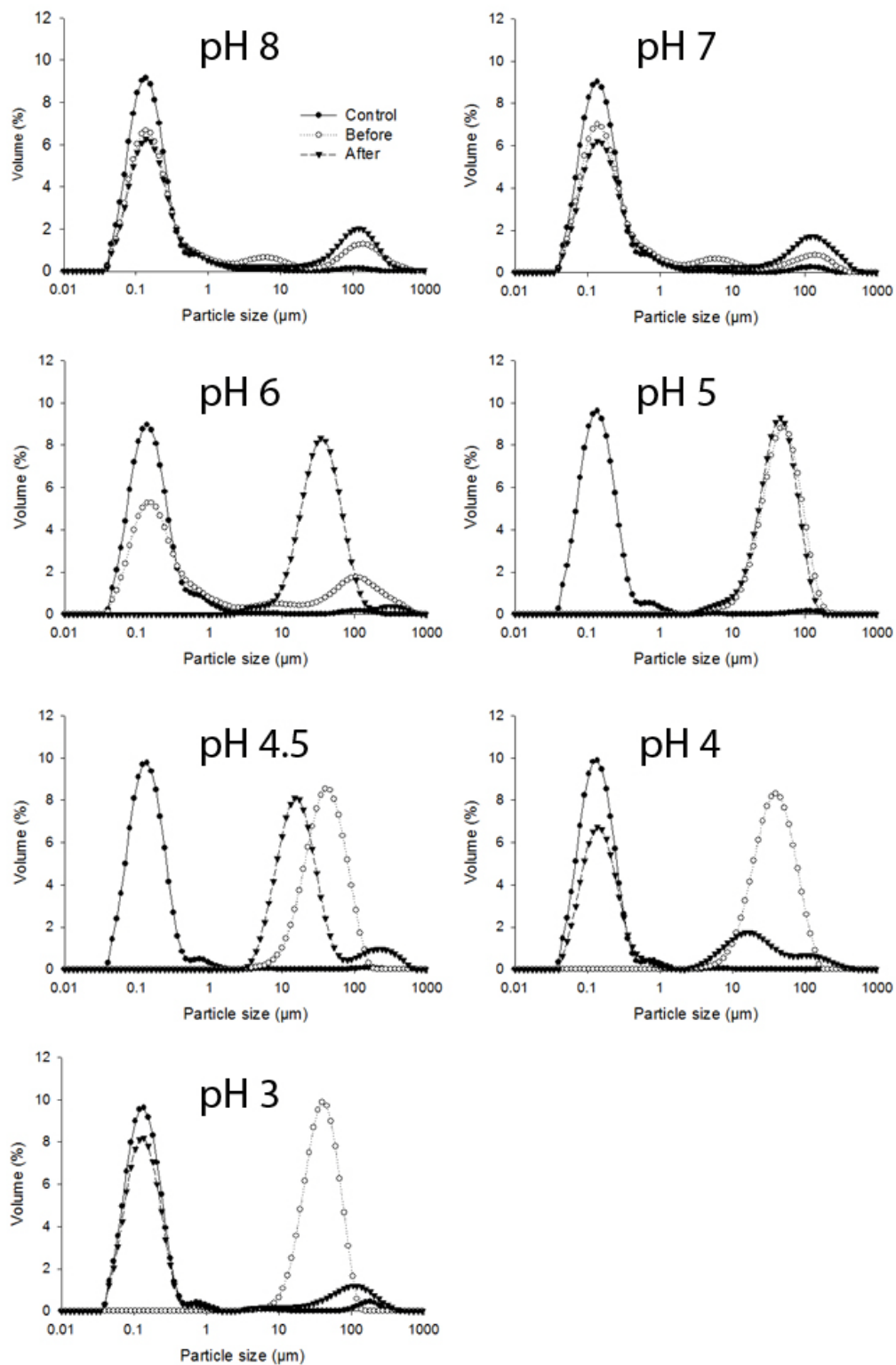


Figure 4.11 – The effect of ionic strength on the particle size distributions of 0.75 wt% SPI + 0.75 wt% SSPS suspensions at pH 3-8.

Table 4.1 shows the effect of pH on the suspension average particle size [D(3,2)] with and without addition of salt. In suspensions with salt added before mixing, there were no significant differences in average particle size between pH 5-3. Suspensions with salt added after mixing showed decreased average particle sizes with decreased pH, correlating with the PSD and sedimentation data above.

Table 4.1 – The effect of 1 wt% NaCl on the average particle sizes of 0.75 wt% SPI + 0.75 wt% SSPS suspensions at pH 3-6 (n = 3).

wt% SSPS / pH	Average particle size [D(3,2)] (μm)				
	6	5	4.5	4	3
Control (0 wt% NaCl)	0.118 ± 0.0	0.112 ± 0.0	0.109 ± 0.0	0.107 ± 0.0	0.108 ± 0.0
1 wt% NaCl added before mixing and pH adjustment	0.198 ± 0.0	33.1 ± 4.0	30.0 ± 7.5	31.9 ± 0.5	29.9 ± 4.7
1 wt% NaCl added after mixing and pH adjustment	24.6 ± 4.6	28.6 ± 2.6	13.7 ± 0.79	0.169 ± 0.0	0.131 ± 0.0

4.4.1.6 Microscopy

pH has a great effect on SPI suspension microstructure (Fig. 4.12). At pH 8, 7, and 6, no aggregation was observed, but at pH 5, 4.5, and 4, near SPI's IEP, the proteins precipitated out of suspension due to charge neutralization, which caused attractive forces to dominate. Protein aggregates were very large (on the order of mm) and existed as large, dense masses. There was some precipitation at pH 3, but much less than at pH 5, 4.5, and 4. The aggregates at pH 3 were smaller in size at ~100 μm. The precipitation of the SPI at pH near its IEP correlated with the sedimentation trends observed for SPI suspensions (Fig. 4.3). No aggregates were observed for SPI suspensions containing SSPS (data not shown), indicating that SSPS was able to stabilize the SPI and prevent its precipitation.

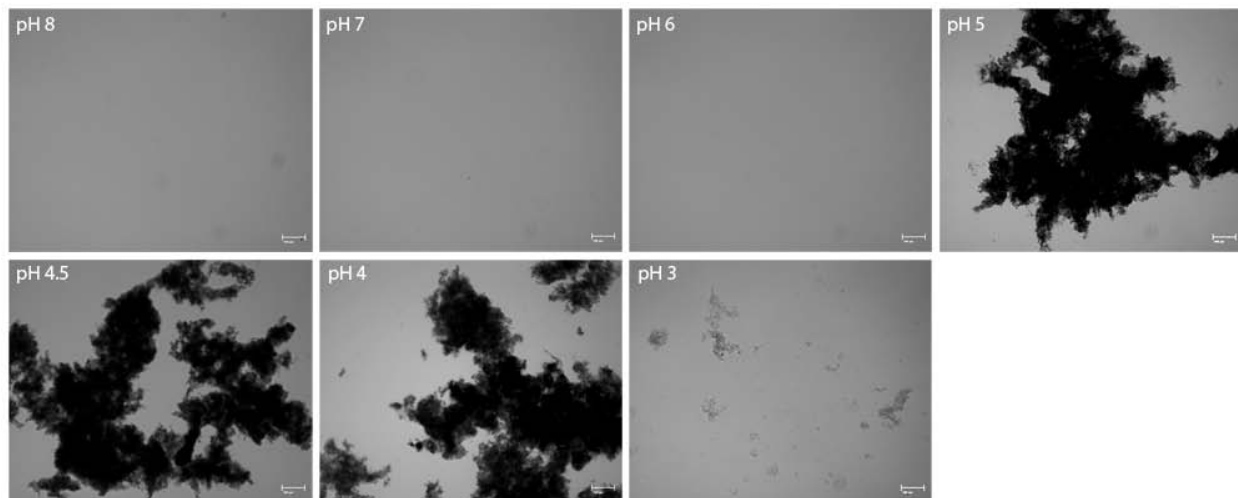


Figure 4.12 – The effect of pH on the microstructure of 0.75 wt% SPI suspensions (bar represents 100 μm).

Fig. 4.13 shows the effect of adding 1 wt% NaCl to 0.75 wt% SPI + 0.75 wt% SSPS suspensions. For suspensions with salt added before mixing and pH adjustment, aggregates were observed for $\text{pH} \leq 5$. The average size of aggregates decreased with decreased pH, corresponding to the sedimentation and particle size data above. Samples with salt added after mixing also corresponded with the sedimentation and particle size data with larger aggregates observed for pH 6 and pH 5. Average aggregate size decreased with pH. It was observed that the aggregates at pH 4.5 and 4 were more translucent than aggregates at higher pH. This might indicate that the aggregates at lower pH were less dense and more loosely-associated than aggregates at higher pH. It was hypothesized that stability increased with decreasing pH because the salt ions had to disrupt more electrostatic bonds between SPI and SSPS before the complexes became dissociated (Fig. 4.10).

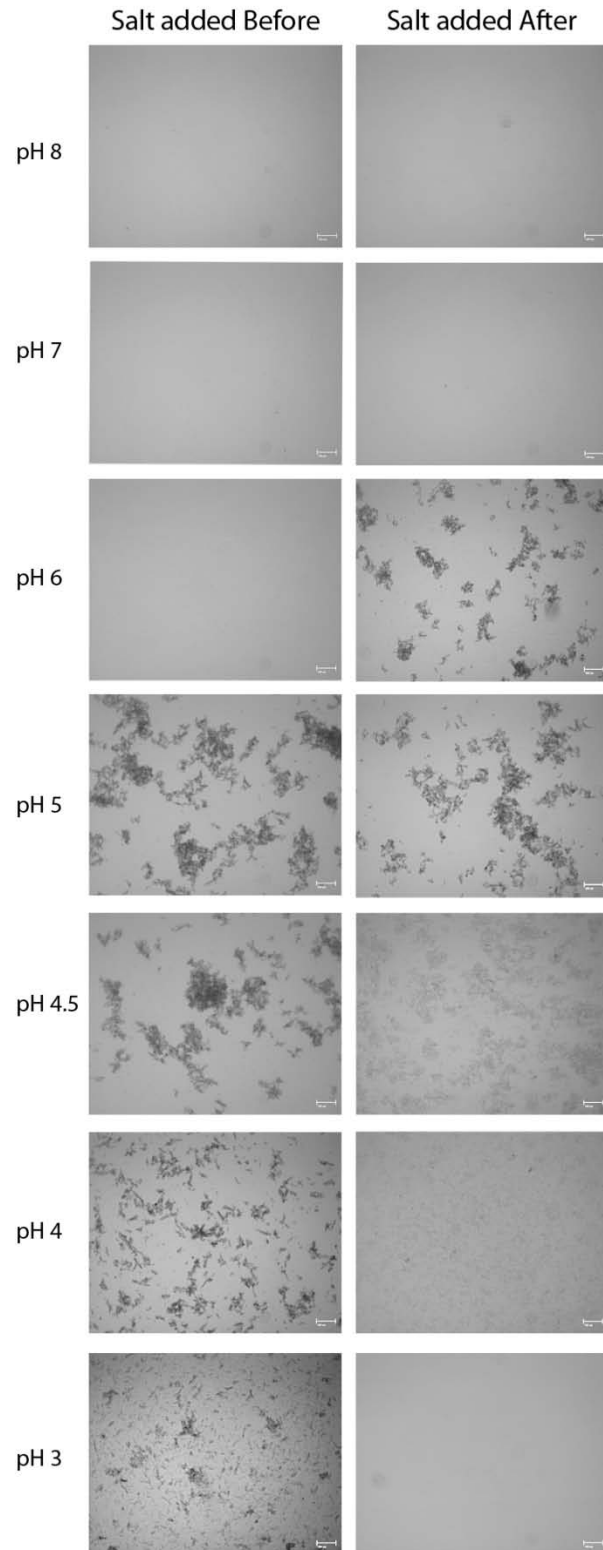


Figure 4.13 – The effect of 1 wt% NaCl on the microstructure of 0.75 wt% SPI + 0.75 wt% SSPS suspensions at various pHs (bar represents 100 μm).

4.4.2 Characterization of SPI-SSPS-stabilized emulsions

Observations from the SPI-SSPS suspensions were directly applicable to SPI-SSPS-stabilized emulsions. The stability of the emulsions studied also greatly depended on the interactions between SPI and SSPS, which in turn were dependent on pH and biopolymer concentrations.

4.4.2.1 Droplet size distributions

Compared to SPI-only systems, emulsion stability was improved in the presence of SSPS (Fig. 4.14 A, C, E, and G). At pH 8 and 7, there were no significant differences between the droplet size distributions (DSDs) of emulsions with and without SSPS, because both SPI and SSPS were negatively-charged, which resulted in electrostatic repulsion. The net negative charges of the biopolymers were sufficiently strong to prevent flocculation and coalescence between SPI-coated droplets. Droplet sizes were smallest at pH 8 and 7. As the pH decreased, droplet sizes increased due to reduced net charges of SPI which allowed for more inter-droplet attractive interactions. The control emulsions (0 wt% SSPS) became destabilized at pH 5, 4.5, and 4, near its IEP, due to isoelectric precipitation of SPI. The addition of ≥ 0.25 wt% SSPS was enough to prevent protein precipitation near SPI's IEP. Increased concentrations of SSPS resulted in shifts to smaller droplet sizes presumably because the higher concentrations of SSPS present at the time of pH adjustment likely bound positive patches of SPI on the droplets more quickly and formed complexes via electrostatic interactions to stabilize them against flocculation and coalescence. Droplet sizes were largest near SPI's IEP (pH 5, 4.5, and 4) and decreased at pH values further from SPI's IEP (pH 6 and 3).

Higher concentrations of SSPS resulted in decreased flocculation and coalescence and had smaller populations at larger droplet sizes (≥ 100 μm) after 28 days of storage (Fig. 4.14 B, D, F, and H). This was probably due to higher concentrations of SSPS providing more complete droplet coverage which improved steric repulsion between droplets which prevented flocculation and coalescence over time. Incomplete droplet coverage at lower SSPS concentrations may have caused bridging flocculation, as was observed by Nakamura *et al.* (2004) for emulsions stabilized by milk whey proteins and SSPS [64]. Increased concentrations of SSPS up to 0.75 wt% did not result in increased average droplet sizes, indicating that SSPS did not induce depletion flocculation, similar to the findings by Roudsari *et al.* (2006) who found that SSPS did not cause depletion flocculation of SPI-stabilized emulsions at concentrations of up to 0.30 wt% (w/v) [76].

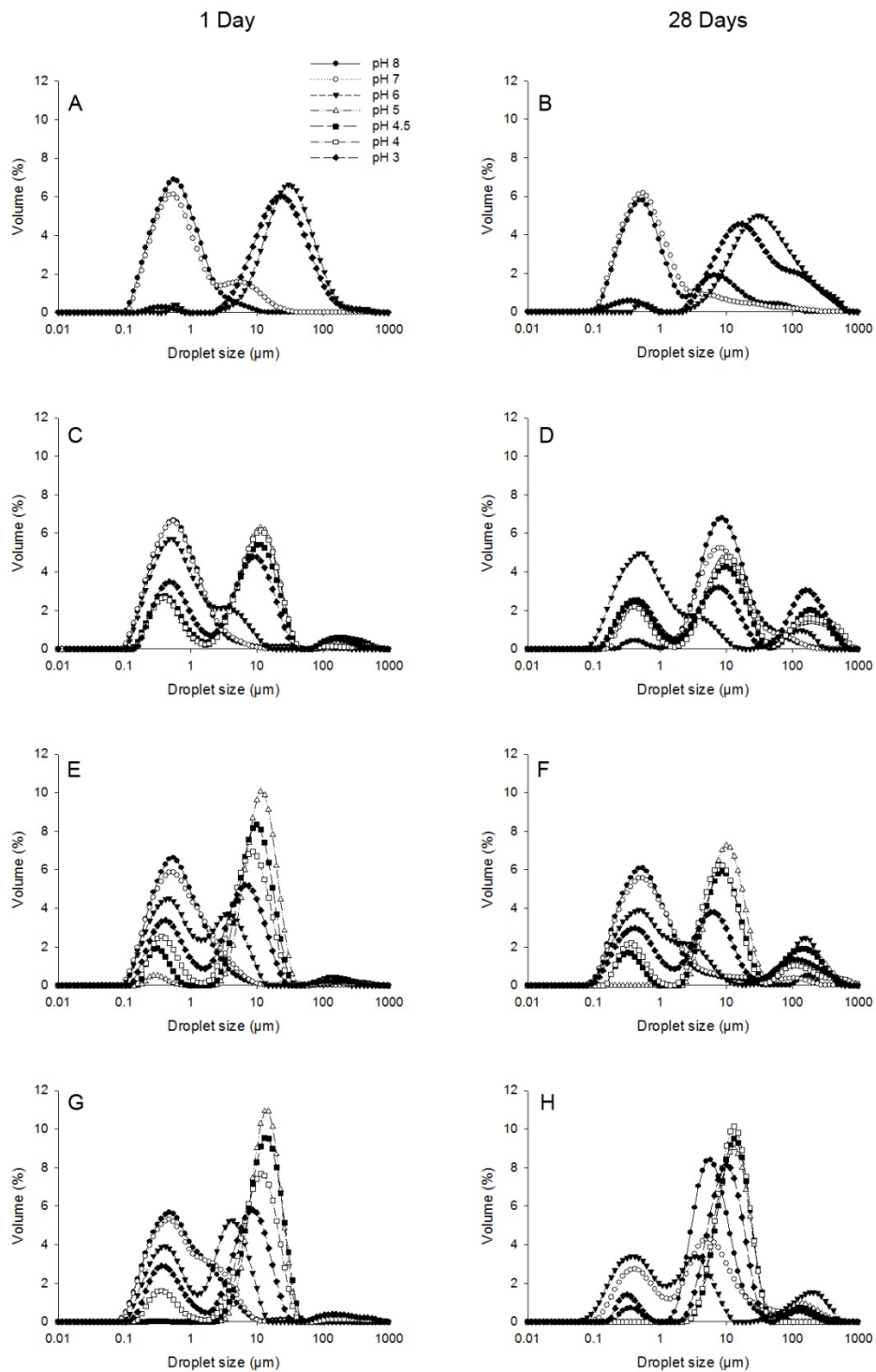


Figure 4.14 – The effect of pH on the droplet size distributions of 0.75 wt% SPI-stabilized emulsions with 0% (A), 0.25 wt% (C), 0.50 wt% (E) and 0.75 wt% SSPS (G) after 1 and 28 days of storage (B, D, F, H, respectively).

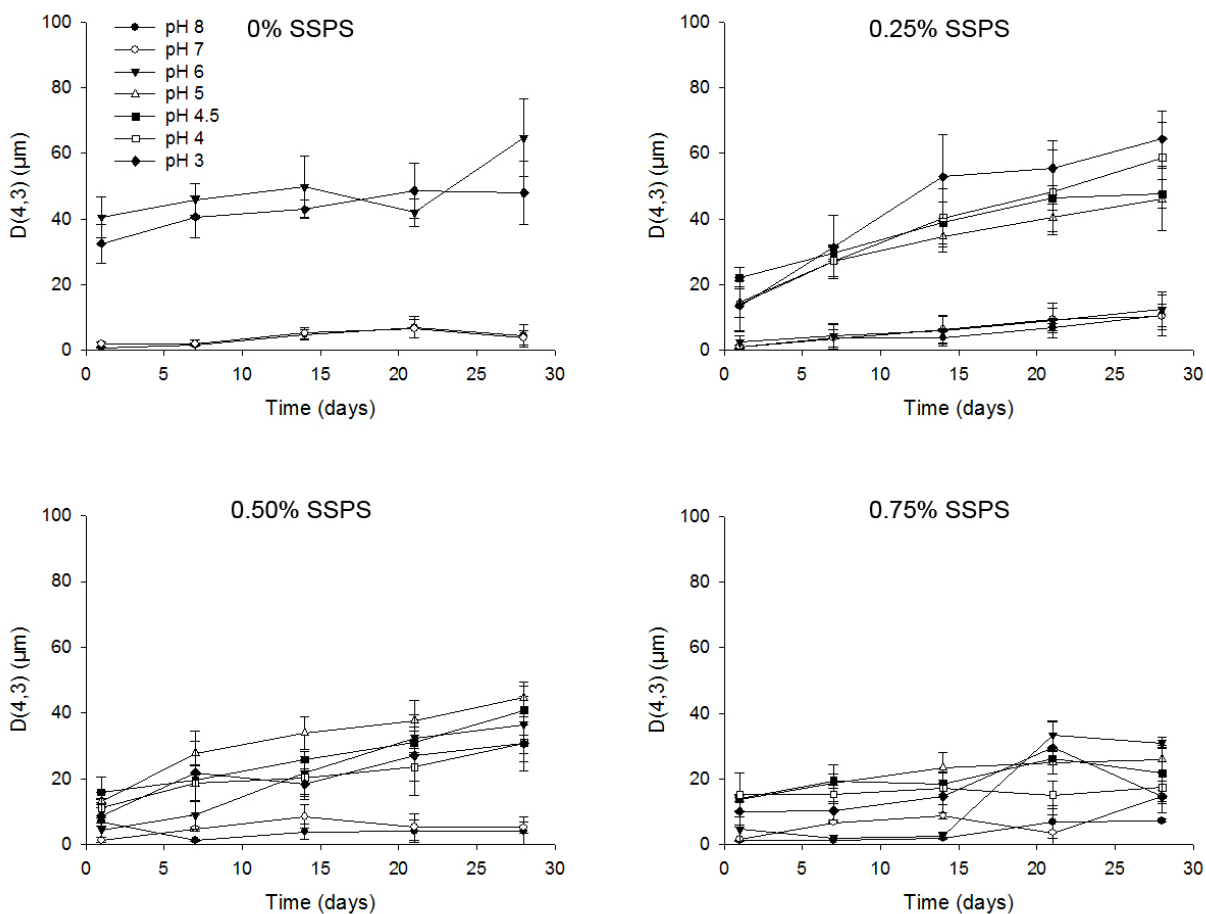


Figure 4.15 – The evolution of average droplet sizes $[D(4,3)]$ over time for 0.75 wt% SPI-stabilized emulsions with varying concentrations of SSPS at: pH 8 (\circ), pH 7 (\bullet), pH 6 (\blacktriangledown), pH 5 (\triangle), pH 4.5 (\blacksquare), pH 4 (\square), and pH 3 (\blacklozenge).

The average droplet sizes $[D(4,3)]$ of the emulsions increased over time with the control emulsions having significantly larger droplets than emulsions stabilized by SSPS ($p \leq 0.05$) (Fig. 4.15). Increasing the concentration of SSPS resulted in smaller droplet sizes with 0.75 wt% SSPS being the most effective at stabilizing droplets against coalescence over time. There were no significant differences in droplet sizes between control emulsions and SSPS-stabilized emulsions at pH 8 and pH 7 due to electrostatic repulsion between droplets because both SPI and SSPS were negatively-charged. Control emulsions (0 wt% SSPS) became destabilized at pHs near the IEP of SPI (pH 5, 4.5, and 4) and so no droplet size measurements could be obtained. For SSPS-stabilized emulsions, average droplet sizes increased at acidic pHs but there were no significant differences in the average droplet sizes between pH 6-3 ($p \leq 0.05$) with the exception of the 0.25 wt% SSPS-stabilized emulsion at pH 6, which had a similar average droplet size those at pH 8 and 7. The

increased stability of emulsion droplets at higher concentrations of SSPS was attributed to increased interactions between the SPI and SSPS that resulted in improved steric barriers against coalescence.

4.4.2.2 Creaming and turbidity

The creaming of SPI-stabilized emulsions was affected by pH. SPI control emulsions exhibited creaming after only one day of storage whereas SPI-SSPS-stabilized emulsions were stable for the entire period of study (28 days). A concentration of 0.25 wt% SSPS was enough to stabilize the 0.75 wt% SPI emulsions (Fig. 4.16 B). Creaming at pH 5, 4.5, and 4 was due to charge neutralization of the proteins at their IEP, correlating with the droplet size data above. This led to phase separation of the emulsions into a clear serum layer depleted of droplets at the bottom and an emulsion layer at the top of the samples (Fig. 4.16 A). The absence of a free oil layer at the top of the emulsion layers indicated that the emulsion droplets did not completely breakdown. This may have been due to the precipitated SPI forming an aggregated network of protein that entrapped the droplets and prevented complete destabilization. Additionally, the emulsion layer volume was relatively large for what was expected if a 5% O/W emulsion became completely destabilized and phase separated. The amount of creaming in control emulsions did not change significantly over time ($p \leq 0.05$). The phase separation behaviour of the emulsions was opposite of that observed for SPI-SSPS suspensions (creaming rather than sedimentation, respectively). This was because the hydrophobic protein aggregates were associated with the oil phase in the emulsion and creamed because the oil had a lower density than water.



Figure 4.16 – The effect of pH on the creaming of 0.75 wt% SPI-stabilized emulsions with 0 wt% (A) and 0.25 wt% (B) SSPS.

The creaming behaviour of the emulsions was further studied via turbidity measurements. The backscattering profiles of samples were used rather than transmission profiles as the relatively high volume fraction of the emulsion droplets reduced the transmitted light to zero, limiting the usefulness of the transmission data [83].

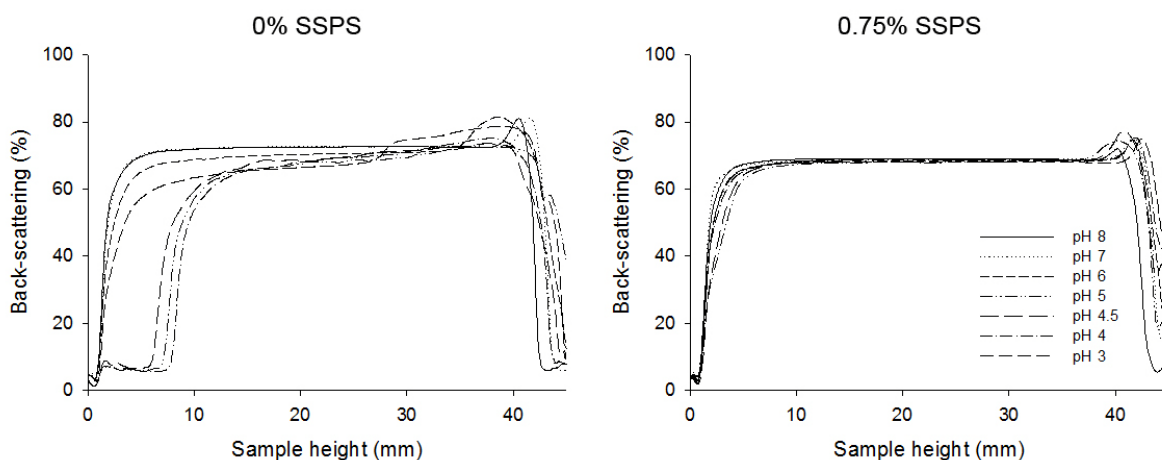


Figure 4.17 – The effect of pH on the back-scattering profiles of 0.75 wt% SPI-stabilized emulsions with and without added SSPS

No creaming was seen for emulsions at pH 8, 7, and 6, which indicated a lack of flocculation and was attributed to sufficient electrostatic repulsion between droplets (Fig. 4.16). Emulsions at pH 3 did not exhibit phase separation upon visual inspection but the backscattering profiles showed a different behavior than emulsions at pH 8, 7, and 6 – the sections below 60% of the total sample height of pH 3 emulsions had ~5% lower backscattering but the top sections had ~5% higher backscattering. This behaviour suggested that the upper layer, having higher backscattering, contained larger droplets than the bottom layer. This contrast in backscattering will hereafter be referred to as *pre-creaming* as the sample exhibited creaming-like behavior but had not undergone visual phase separation. Overall, the addition of SSPS resulted in increased emulsion stability against creaming as well as pre-creaming with increased concentrations of SSPS (up to 0.75 wt%) resulting in increased stability for the entire period of study (28 days) ($p \leq 0.05$).

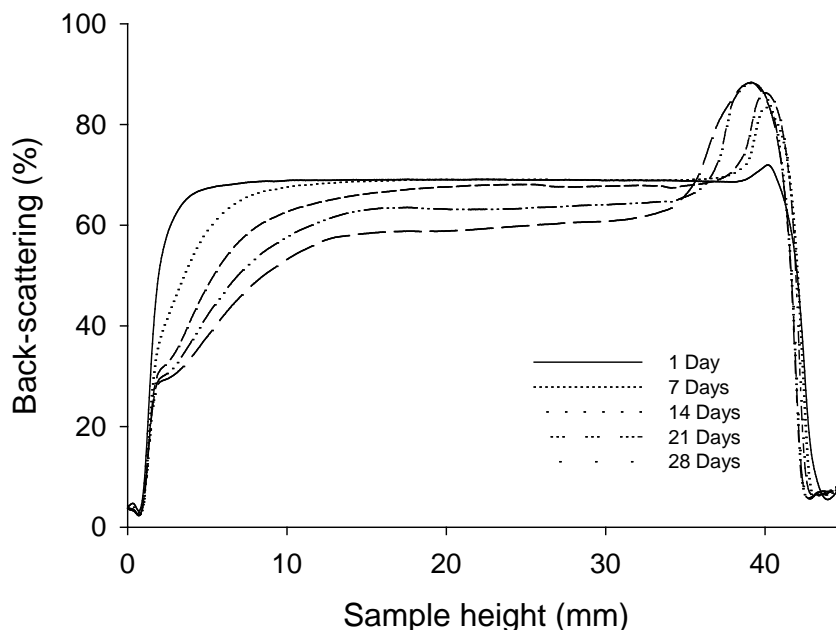


Figure 4.18 – The evolution of the back-scattering profile of a 0.75 wt% SPI + 0.75 wt% SSPS emulsion at pH 8 over time.

The backscattering profiles of the emulsions changed over time (Fig. 4.18). Lower regions of the sample decreased in backscattering intensity over time, indicating a decrease in average droplet size due to the larger droplets having migrated towards the top of the sample due to oil having a lower density than water. This caused in an increase in backscattering at the top of the sample. The

migration of droplets over time led to gradual clearing at the bottom of the sample and a thickening at the top. This pre-creaming was observed for control emulsions as well as SSPS-stabilized emulsions at all pH values tested. The rates of clearing and pre-creaming over time were measured (Table 4.2 and 4.3).

Table 4.2 – Evolution of clearing rates for 0.75 wt% SPI-stabilized emulsions with various concentrations of SSPS.

Rates of clearing at bottom of samples (measurement height = 3 mm) (Δ BS%/day)							
wt% SSPS/pH	8	7	6	5	4.5	4	3
0	-0.96	-1.19	-1.10	N/A*	N/A*	N/A*	-1.11
	± 0.4	± 0.1	± 0.0				± 0.2
0.25	-1.36	-1.28	-1.36	-0.86	-1.18	-0.96	-1.08
	± 0.1	± 0.1	± 0.1	± 0.1	± 0.2	± 0.0	± 0.0
0.50	-1.53	-1.38	-0.96	-0.90	-1.06	-1.19	-0.85
	± 0.1	± 0.4	± 0.5	± 0.2	± 0.3	± 0.1	± 0.3
0.75	-1.12	-1.24	-0.75	-0.81	-0.90	-1.06	-0.56
	± 0.4	± 0.4	± 0.1	± 0.2	± 0.6	± 0.2	± 0.1

*Emulsion was unstable and exhibited phase separation.

Table 4.3 – Evolution of pre-creaming rates for 0.75 wt% SPI-stabilized emulsions with various concentrations of SSPS.

Rates of pre-creaming at the top of samples (measurement height = 40 mm) (Δ BS%/day)							
wt% SSPS/pH	8	7	6	5	4.5	4	3
0	0.61	0.64	0.22	N/A*	N/A*	N/A*	0.21
	± 0.2	± 0.1	± 0.2				± 0.0
0.25	0.81	0.76	0.83	0.59	0.92	0.62	0.83
	± 0.0	± 0.0	± 0.1	± 0.1	± 0.1	± 0.1	± 0.0
0.50	0.78	0.70	0.45	0.22	0.23	0.53	0.41
	± 0.0	± 0.2	± 0.3	± 0.1	± 0.1	± 0.2	± 0.1
0.75	0.76	0.72	0.63	0.26	0.18	0.09	0.23
	± 0.1	± 0.0	± 0.0	± 0.0	± 0.1	± 0.0	± 0.1

*Emulsion was unstable and exhibited phase separation.

There were no significant differences in the rates of clearing for all emulsions at pH 8 and pH 7 due to control and SSPS-stabilized emulsions having the same droplet sizes (Fig. 4.13), which affects the rate of droplet migration (Eqn. 1.2). Control emulsions showed higher rates of clearing at pH 6 and pH 3 compared to SSPS-stabilized emulsions due to larger droplet sizes. There was no difference in clearing rates with increased concentrations of SSPS ($p \leq 0.05$). Pre-creaming rates at the top of the samples followed the same general trend: there was no difference between the pre-creaming rates of control emulsions and SSPS-stabilized emulsions at pH 8 and 7 but higher concentrations of SSPS showed lower creaming rates at acidic pH ($p \leq 0.05$). Emulsions stabilized with 0.75 wt% SSPS had the smallest droplet sizes (Fig. 4.14) and therefore exhibited the least pre-creaming.

4.4.2.3 Microscopy

The presence of SSPS and pH had a significant effect on emulsion stability (Fig. 4.19). Control emulsions were stable at pH 8 and pH 7 due to electrostatic repulsion between negatively-charged SPI and SSPS, but became increasingly destabilized as pH decreased which caused a decrease in SPI's overall charge. This resulted in increased inter-droplet interactions and led to flocculation, aggregation, and coalescence with emulsion destabilization greatest at pHs near SPI's IEP. This correlated with the DSD and creaming data discussed above. Addition of SSPS stabilized the emulsions against flocculation over the entire pH range studied with higher amounts of SSPS resulting in the lowest amount of flocculation (Fig. 4.19 - only images of 0.75 wt% SSPS-stabilized emulsions are shown for clarity).

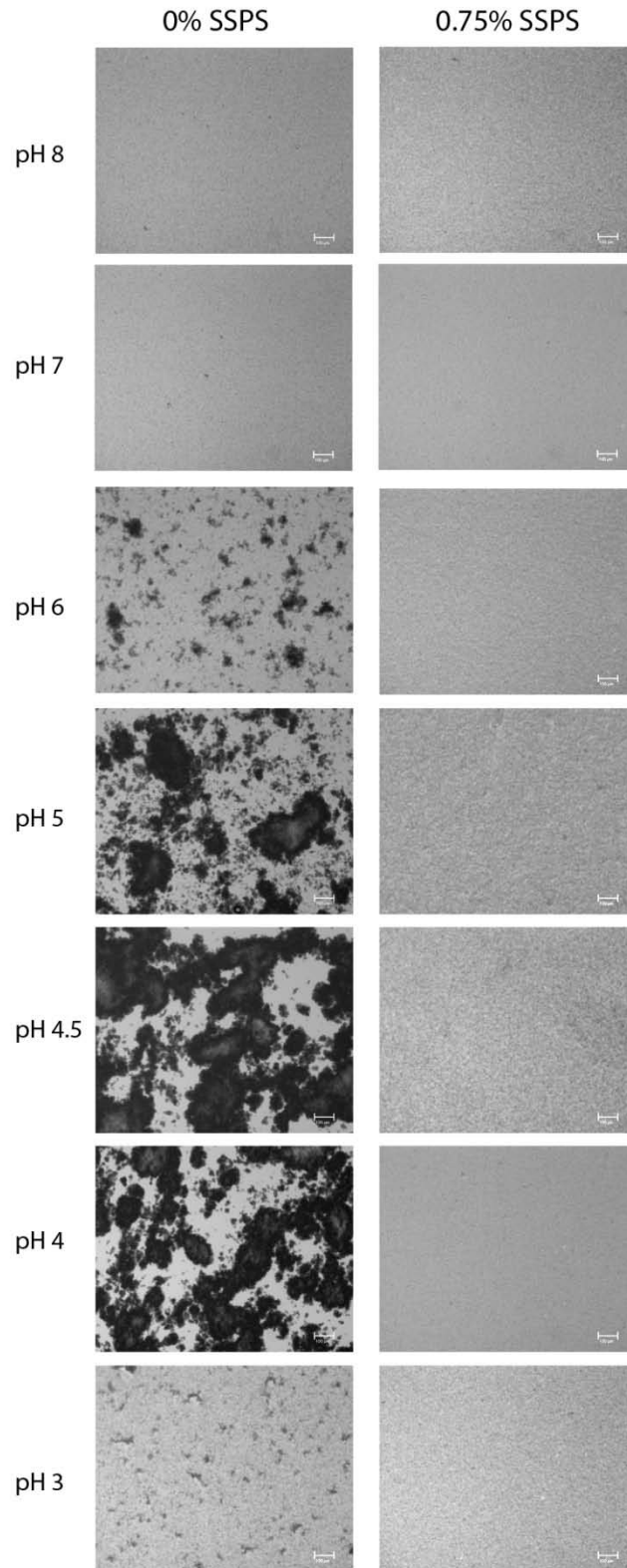


Figure 4.19 – The effect of pH on the microstructure of 0.75 wt% SPI-stabilized emulsions with and without SSPS (bar represents 100 μm).

4.5 Conclusions

The stability of SPI in suspension greatly depended on pH, the presence of SSPS, and ionic strength. Suspensions of 0.75 wt% SPI became destabilized at moderately acidic pH due to decreased solubility resulting from protein charge neutralization. This was overcome through the addition of ≥ 0.25 wt% SSPS, which formed complexes with the SPI via electrostatic interactions. Surface charge measurements indicated that SPI-SSPS complexes had zeta potentials of 0 mV yet they remained soluble and stable against aggregation, suggesting that SSPS stabilized SPI *via* steric rather than electrostatic repulsion. The stabilizing effects of SSPS on SPI suspensions were confirmed by the lack of sedimentation as well as the absence of aggregation as observed *via* microscopy. The stability of the complexes depended on the ionic strength of the suspensions with increased ionic strengths resulting in decreased stability presumably due to charge screening by the salt ions which prevented or decreased interaction between the proteins and polysaccharide and promoted self-association.

The interaction of SPI and SSPS also affected the stability of O/W emulsions. These interactions were governed by pH and biopolymer concentration. In the absence of SSPS, emulsion stability decreased with decreasing pH due to charge neutralization of SPI which caused increased flocculation and coalescence. A minimum of 0.25 wt% SSPS was required to stabilize 5.0 wt% O/W emulsions containing 0.75 wt% SPI at moderately acidic conditions for up to 28 days. Increased SSPS concentrations (up to 0.75 wt%) resulted in smaller droplet sizes which improved emulsion stability against creaming and pre-creaming. Microscopy images showed that SSPS was crucial to stabilize the emulsions under acidic conditions.

Chapter 5 – Overall Conclusions

Dispersed protein and polysaccharide systems may become destabilized via sedimentation or creaming which can lead to flocculation and eventually aggregation or coalescence, for aqueous suspensions or emulsions, respectively. The stability of these dispersed systems depends on environmental conditions such as pH, ionic strength, and the concentrations of stabilizing agents such as proteins and polysaccharides. The overall net charge of proteins depends on pH and the stability of protein-stabilized dispersed systems is lowest when the proteins are at or near their IEP. This is due to a reduction in the efficacy of electrostatic repulsion between particles or droplets which results in increased flocculation/aggregation. Stability can be improved by electrostatically complexing the proteins with a polysaccharide that provides electrostatic and/or steric repulsion. This occurs at pHs below the IEP of the proteins but above that of the polysaccharides where the proteins and polysaccharides are oppositely-charged. Ionic strength also affects complexation, as higher concentrations of salt may cause charge-screening of the proteins and polysaccharides and inhibit electrostatic interactions, which may reduce or prevent complexation. Stability is greatest when the concentration of polysaccharide is sufficiently high to fully cover protein surfaces to form cohesive layers. These principles apply to both aqueous suspensions and oil-in-water emulsions.

Chapter 6 – Future Studies

Areas for further study include the following:

- i. Studying the surface charge of emulsion systems. Our zeta potential analyzer is capable of measuring the zeta potential of smaller particles ($\leq 30 \mu\text{m}$), but it can measure larger particles if their density is matched to that of the solvent's or the medium's viscosity is increased. This can be achieved by using brominated oils that have densities similar to water or adding in non-interacting thickening agents, respectively.
- ii. Studying the effect of increased ionic strength on SPI-SSPS-stabilized emulsions. It is hypothesized that the emulsions would behave in a similar manner to SPI-SSPS-stabilized suspensions in that upon the addition of salt, the SPI-SSPS emulsions would become destabilized due to electrostatic screening effects that disrupt and prevent protein-polysaccharide complexation. This may be pH-dependent, as seen for the suspensions, where at lower pH values the emulsions may be stable. One can also examine and compare the effects of multivalent ions on the stability of SPI-SSPS suspensions and emulsions to the results obtained for monovalent ions.
- iii. Studying emulsion destabilization via addition of enzymes. If these SPI-SSPS suspensions or emulsions system are to be adapted for food applications, it is important to understand the effects of digestive enzymes on their stability. This can be done using simulated gastric fluids or digestive tracts.
- iv. Encapsulating a nutraceutical or pharmaceutical and studying its release. The encapsulation and controlled release of nutraceuticals and pharmaceuticals is becoming increasingly popular with the drive to fortify food products and make them healthier. To study the encapsulation and release of a lipophilic model molecule, one can incorporate it into the oil phase before it is dispersed. One can then instigate destabilization of the system by adjusting the pH or ionic strength to reverse SPI-SSPS complexation and measure the release of the model molecule over time. One can also subject a model molecule-loaded emulsion to enzymatic degradation to cause release.

Chapter 7 – References

1. Schramm, L.L., *Emulsions, Foams, and Suspensions: Fundamentals and Applications*. 2005, Weinheim, Germany: Wiley-VCH.
2. Molina-Bolivar, J.A., Galisteo-Gonzalez, F., and Hidalgo-Alvarez, R., *Colloidal stability of protein-polymer systems: A possible explanation by hydration forces*. *Physical Review E*, 1997. **55**(4): p. 4522-4530.
3. Benichou, A., Aserin, A., and Garti, N., *O/W/O double emulsions stabilized with WPI-polysaccharide conjugates*. *Colloids and Surfaces A: Physicochem. Eng. Aspects*, 2006. **297**: p. 211-220.
4. Qi, X., Wang, L., Zhu, J., Hu, Z., and Zhang, J., *Self-double-emulsifying drug delivery system (SDEDDS): a new way for oral delivery of drugs with high solubility and low permeability*. *International Journal of Pharmaceutics*, 2011. **409**: p. 245-251.
5. Friberg, S.E., Larsson, K., and Sjoblom, J., ed. *Food Emulsions: Fourth edition, revised, and expanded*. 4 ed. 2004.
6. Dalgleish, D.G., *Adsorption of protein and stability of emulsions*. *Trends in Food Science & Technology*, 1997. **8**: p. 1-6.
7. Ettelaie, R., Akinshina, A., and Dickinson, E., *Mixed protein-polysaccharide interfacial layers: a self consistent field calculation study*. *Faraday Discuss.*, 2008. **139**: p. 161-178.
8. Sjoblom, J., *Emulsions and Emulsion Stability*. 1996, New York, USA: Marcel Dekker, Inc.
9. Jimenez-Colmenero, F., Herrero, A., Pintado, T., Solas, M.T., and Ruiz-Capillas, C., *Influence of emulsified olive oil stabilizing system used for pork backfat replacement in frankfurters*. *Food Research International*, 2010. **43**: p. 2068-2076.
10. McClements, D.J., *Understanding and controlling the microstructure of complex foods*. 2007, Cambridge, England: Woodhead Publishing Limited.
11. Benichou, A., Aserin, A., and Garti, N., *Protein-polysaccharide interactions for stabilization of food emulsions*. *J. Dispersion Science and Technology*, 2002. **23**(1-3): p. 93-123.
12. Tolstoguzov, V.B., *Functional properties of food proteins and role of protein-polysaccharide interaction*. *Food Hydrocolloids*, 1991. **4**(6): p. 429-468.
13. Grinberg, V.Y. and Tolstoguzov, V.B., *Thermodynamic incompatibility of proteins and polysaccharides in solutions*. *Food Hydrocolloids*, 1997. **11**(2): p. 145-158.
14. Perez, A.A., Carrara, C.R., Sanchez, C.C., Patino, J.M.R., and Santiago, L.G., *Interactions between milk whey protein and polysaccharide in solution*. *Food Chemistry*, 2009. **116**: p. 104-113.
15. Sanchez, C., Schmitt, C., Babak, V.G., and Hardy, J., *Rheology of whey protein isolate-xanthan mixed solutions and gels. Effect of pH and xanthan concentration*. *Nahrung*, 1997. **41**(6): p. 336-343.
16. Shih, F.F., *Interaction of soy isolate with polysaccharide and its effect on film properties*. *JAOCs*, 1994. **71**(11): p. 1281-1285.
17. Becher, P., *Emulsions: Theory and Practice*. 2001, Washington, D.C., USA: Oxford University Press.
18. McClements, D.J., *Protein-stabilized emulsions*. *Current Opinion in Colloid & Interface Science*, 2004. **9**: p. 305-313.
19. Palazolo, G.G., Sobral, P.A., and Wagner, J.R., *Freeze-thaw stability of oil-in-water emulsions prepared with native and thermally-denatured soybean isolates*. *Food Hydrocolloids*, 2011. **25**: p. 398-409.
20. Martinez, K.D., Ganesan, V., Pilosof, A.M.R., and Harte, F.M., *Effect of dynamic high-pressure treatment on the interfacial and foaming properties of soy protein isolate-hydroxymethylcelluloses systems*. *Food Hydrocolloids*, 2011. **25**: p. 1640-1645.

21. Puppo, M.C., Beaumal, V., Speroni, F., de Lamballerie, M., Anon, M.C., and Anton, M., *Beta-conglycinin and glycinin soybean protein emulsions treated by combined temperature-high pressure treatment*. Food Hydrocolloids, 2011. **25**: p. 389-397.
22. Jiang, J., Xiong, Y.L., and Chen, J., *pH Shifting alters solubility characteristics and thermal stability of soy protein isolate and its globulin fractions in different pH, salt concentration, and temperature conditions*. J. Agric. Food chem., 2010. **58**: p. 8035-8042.
23. Grigoriev, D.O. and Miller, R., *Mono- and multilayer covered drops as carriers*. Current Opinion in Colloid & Interface Science, 2009. **14**: p. 48-59.
24. Xu, Q., Nakajima, M., Liu, Z., and Shiina, T., *Soybean-based surfactants and their applications*. InTech, 2011: p. 341-364.
25. Chen, L., Chen, J., Ren, J., and Zhao, M., *Modifications of soy protein isolates using combined extrusion pre-treatment and controlled enzymatic hydrolysis for improved emulsifying properties*. Food Hydrocolloids, 2011. **25**: p. 887-897.
26. Moure, A., Sineiro, J., Dominguez, H., and Parajo, J.C., *Functionality of oilseed protein products: A review*. Food Research International, 2006. **39**: p. 945-963.
27. Dickinson, E., *Colloid science of mixed ingredients*. Soft Matter, 2006. **2**(642-652).
28. Manion, B. and Corredig, M., *Interactions between Whey Protein Isolate and Soy Protein Fractions at Oil-Water interfaces: Effects of heat and concentration of protein in the aqueous phase*. Journal of Food Science, 2006. **71**(8): p. 343-349.
29. Staswick, P.E., Hermodson, M.A., and Nielson, N.C., *Identification of the cystines which link the acidic and basic components of the glycinin subunits*. The Journal of Biological Chemistry, 1984. **259**(21): p. 13431-13435.
30. Lakemond, C.M.M., de Jongh, H.H.J., Hessing, M., Gruppen, H., and Voragen, A.G.J., *Heat denaturation of soy glycinin: influence of pH and ionic strength on molecular structure*. J. Agric. Food Chem., 2000. **48**: p. 1991-1995.
31. Lam, M., Shen, R., Paulsen, P., Corredig, M., *Pectin stabilization of soy protein isolates at low pH*. Food Research International, 2006. **40**: p. 101-110.
32. Shen, J.L., *Solubility profile, intrinsic viscosity, and optical rotation studies of acid precipitated soy protein and of commercial soy isolate*. J. Agric. Food Chem., 1976. **24**(4): p. 784-788.
33. Kunz, W., Henle, J., and Ninham, B.W., *'Zur Lehre von der Wirkung der Salze' (about the science of the effect of salts): Franz Hofmeister's historical papers*. Current Opinion in Colloid & Interface Science, 2004. **9**: p. 19-97.
34. Gibb, C.L.D., and Gibb, B.C., *Anion binding to hydrophobic concavity is central to the salting-in effects of Hofmeister chaotropes*. J. Am. Chem. Soc., 2011. **133**: p. 7344-7347.
35. Chen, W.S. and Soucie, W.G., *The ionic modification of the surface charge and isoelectric point of soy protein*. JAOCS, 1986. **63**(10): p. 1346-1350.
36. Lakemond, C.M.M., de Jongh, H.H.J., Hessing, M., Gruppen, H., and Voragen, A.G.J., *Soy glycinin: influence of pH and ionic strength on solubility and molecular structure at ambient temperatures*. Journal of Agricultural and Food Chemistry, 2000. **48**(6): p. 1985-1990.
37. German, B., Damodaran, S., and Kinsella, J.E., *Thermal dissociation and association behavior of soy proteins*. J. Agric. Food Chem., 1982. **30**: p. 807-811.
38. Keerati-u-rai, M. and Corredig, M., *Heat-induced changes occurring in oil/water emulsions stabilized by soy glycinin and beta-conglycinin*. J. Agric. Food Chem., 2010. **58**: p. 9171-9180.
39. Iwabuchi, S., Watanabe, H., and Yamauchi, F., *Observations on the dissociation of beta-conglycinin into subunits by heat treatment*. J. Agric. Food Chem., 1991. **39**: p. 34-40.
40. Zhang, H., Li, L., and Mittal, G.S., *Effects of high pressure processing on soybean beta-conglycinin*. Journal of Food Process Engineering, 2010. **33**: p. 568-583.
41. Puppo, C., Chapleau, N., Speroni, F., de Lamballerie-Anton, M., Michel, F., Anon, C., and Anton, M., *Physicochemical modifications of high-pressure-treated soybean protein isolates*. J. Agric. Food Chem., 2004. **52**: p. 1564-1571.

42. Tang, C. and Ma, C., *Effect of high pressure treatment on aggregation and structural properties of soy protein isolate*. Food Science and Technology, 2009. **42**: p. 606-611.
43. Molina, E., Papadopoulou, A., and Ledward, D.A., *Emulsifying properties of high pressure treated soy protein isolate and 7S and 11S globulins*. Food Hydrocolloids, 2000. **15**: p. 263-269.
44. Mitidieri, F.E. and Wagner, J.R., *Coalescence of o/w emulsions stabilized by whey and isolate soybean proteins. Influence of thermal denaturation, salt addition, and competitive interfacial adsorption*. Food Research International, 2002. **35**: p. 547-557.
45. Palazolo, G.G., Mitidieri, F.E., and Wagner, J.R., *Relationship between interfacial behaviour of native and denatured soybean isolates and microstructure and coalescence of oil in water emulsions - effect of salt and protein concentration*. Food Sci Tech Int, 2003. **9**(6): p. 409-419.
46. Aoki, H., Taneyama, O., and Inami, M., *Emulsifying properties of soy protein: characteristics of 7S and 11S proteins*. Journal of Food Science, 1980. **45**: p. 534-546.
47. Hwang, J.K., Kim, Y.S., and Pyun, Y.R., *Comparison of the effect of soy protein isolate concentration on emulsion stability in the absence or presence of monoglyceride*. Food Hydrocolloids, 1991. **5**(3): p. 313-317.
48. Liu, C., Yang, X., Ahmad, I., Tang, C., Li, L., Zhu, J., and Qi, J., *Rheological properties of soybean beta-conglycinin in aqueous dispersions: effects of concentration, ionic strength, and thermal treatment*. International Journal of Food Properties, 2011. **14**: p. 264-279.
49. Luo, D., Zhao, Q., Zhao, M., Yang, B., Long, X., Ren, J., and Zhao, H., *Effects of limited proteolysis and high-pressure homogenisation on structural and functional characteristics of glycinin*. Food Chemistry, 2010. **122**: p. 25-30.
50. Radha, C., Kumar, P.R., and Prakash, V., *Enzymatic modification as a tool to improve the functional properties of heat-processed soy flour*. Journal of the Science of Food and Agriculture, 2008. **88**: p. 336-343.
51. Dickinson, E., Goller, M.I., and Wedlock, D.J., *Osmotic pressure, creaming, and rheology of emulsions containin nonionic polysaccharide*. Journal of Colloid and Interface Science, 1995. **172**: p. 192-202.
52. Ray, A.K., Bird, P.B., Iacobucci, G.A., and Clark, B.C. Jr, *Functionality of gum arabic. Fractionation, characterization and evaluation of gum fractions in citrus oil emulsions and model beverages*. Food Hydrocolloids, 1995. **9**(2): p. 123-131.
53. Nakamura, A., Furuta, H., Kato, M., Maeda, H., and Nagamatsu, Y., *Effect of soybean soluble polysaccharides on the stability of milk protein under acidic conditions*. Food Hydrocolloids, 2003. **17**: p. 333-343.
54. Nakamura, A., Yoshida, R., Maeda, H., Furuta, H., and Corredic, M., *Study of the role of the carbohydrate and protein moieties of soy soluble polysaccharides in their emulsifying properties*. J. Agric. Food Chem., 2004. **52**: p. 5506-5512.
55. McNamee, B.F., O'Riordan, E.D., and O'Sullivan, M., *Emulsification and microencapsulation properties of gum arabic*. J. Agric. Food Chem., 1998. **46**: p. 4551-4555.
56. Buffo, R.A., Reineccius, G.A., and Oehlert, G.W., *Factors affecting the emulsifying and rheological properties of gum acacia in beverage emulsions*. Food Hydrocolloids, 2001. **15**: p. 53-66.
57. Islam, A.M., Phillips, G.O., Slijivo, A., Snowden, M.J., and Williams, P.A., *A review of recent developments on the regulatory, structural and functional aspects of gum arabic*. Food Hydrocolloids, 1997. **11**(4): p. 493-505.
58. Mun, S., Choi, Y., Shim, J., Park, K., and Kim, Y., *Effects of enzymatically modified starch on the encapsulation efficiency and stability of water-in-oil-in-water emulsions*. Food Chemistry, 2011. **128**: p. 266-275.
59. Garti, N., *Hydrocolloids as emulsifying agents for oil-in-water emulsions*. J. Dispersion Science and Technology, 1999. **20**(1 & 2): p. 327-355.

60. Nakamura, A., Takahashi, T., Yoshida, R., Maeda, H., and Corredig, M., *Emulsifying properties of soybean soluble polysaccharide*. Food Hydrocolloids, 2004. **18**: p. 795-803.
61. Nakamura, A., Yoshida, R., Maeda, H., Corredig, M., *Soy soluble polysaccharide stabilization at oil-water interfaces*. Food Hydrocolloids, 2006. **20**: p. 277-283.
62. Furuta, H. and Maeda, H., *Rheological properties of water-soluble soybean polysaccharides extracted under weak acidic condition*. Food Hydrocolloids, 1999. **13**: p. 267-274.
63. Nakamura, A., Maeda, H., and Corredig, M., *Emulsifying properties of enzyme-digested soybean soluble polysaccharide*. Food Hydrocolloids, 2006. **20**: p. 1029-1038.
64. Nakamura, A., Maeda, H., and Corredig, M., *Competitive adsorption of soy soluble polysaccharides in oil-in-water emulsions*. Food Research International, 2004. **37**: p. 823-831.
65. Nakamura, A., Maeda, H., and Corredig, M., *Influence of heating on oil-in-water emulsions prepared with soybean soluble polysaccharide*. J. Agric. Food Chem., 2007. **55**: p. 502-509.
66. Dickinson, E., *Hydrocolloids at interfaces and the influence on the properties of dispersed systems*. Food Hydrocolloids, 2003. **17**: p. 25-39.
67. Samant, S.K., Singhal, R.S., Kulkarni, P.R., and Rege, D.V., *Protein-polysaccharide interactions: a new approach in food formulations*. International Journal of Food Science and Technology, 1993. **28**: p. 547-562.
68. Schmitt, C., Sanchez, C., Desobry-Banon, S., and Hardy, J., *Structure and technofunctional properties of protein-polysaccharide complexes: a review*. Critical Reviews in Food Science and Nutrition, 1998. **38**(8): p. 689-753.
69. Miquelim, J.N., Lannes, S.C.S., and Mezzenga, R., *pH Influence on the stability of foams with protein-polysaccharide complexes at their interfaces*. Food Hydrocolloids, 2010. **24**: p. 398-405.
70. Koupantsis, T. and Kiosseoglou, V., *Whey protein-carboxymethylcellulose interaction in solution and in oil-in-water emulsion systems. Effect on emulsion stability*. Food Hydrocolloids, 2009. **23**: p. 1156-1163.
71. Liu, J., Verespej, E., Alexander, M., and Corredig, M., *Comparison on the effect of high-methoxyl pectin or soybean-soluble polysaccharide on the stability of sodium caseinate-stabilized oil/water emulsions*. J. Agric. Food Chem., 2007. **55**: p. 6270-6278.
72. Liu, J., Nakamura, A., and Corredig, M., *Addition of pectin and soy soluble polysaccharide affects the particle size distribution of casein suspensions prepared from acidified skim milk*. J. Agric. Food Chem., 2006. **54**: p. 6241-6246.
73. Martinez, K.D., Sanchez, C.C., Ruiz-Henestrosa, V.P., Patino, J.M.R., and Pilosof, A.M.R., *Soy protein-polysaccharide interactions at the air-water interface*. Food Hydrocolloids, 2007. **21**: p. 804-812.
74. Giancone, T., Torrieri, E., Masi, P., Michon, C., *Protein-polysaccharide interactions: phase behaviour of pectin-soy flour mixture*. Food Hydrocolloids, 2009. **23**: p. 1263-1269.
75. Lam, M., Paulsen, P., and Corredig, M., *Interactions of soy protein fractions with high-methoxyl pectin*. J. Agric. Food Chem., 2008. **56**: p. 4726-4735.
76. Roudsari, M., Nakamura, A., Smith, A., and Corredig, M., *Stabilizing behavior of soy soluble polysaccharide or high methoxyl pectin in soy protein isolate emulsions at low pH*. J. Agric. Food Chem., 2006. **54**: p. 1434-1441.
77. Kinematica AG, *Polytron Dispersing and Mixing Technology and Pilot Plant Systems POLYTRON PT-K and PT-G*, Kinematica AG: Lucerne, Switzerland.
78. APV, *APV Lab Series Homogenizers: 1000/2000 series*. 2008.
79. Malvern Instruments Limited, *Mastersizer 2000: Integrated systems for particle sizing*. 2005: Worcestershire, UK.
80. Malvern Instruments Limited, *Mastersizer 2000 user manual*. 2007, England.

81. Gregory, J., *Monitoring particle aggregation processes*. Advances in Colloid and Interface Science, 2009. **147-148**: p. 109-123.
82. Corporation, B.I., *ZetaPlus Zeta Potential Analyzer Instruction Manual*. 2003.
83. Formulation, *Turbiscan LAB User Manual*. 2006.
84. Puppo, M.C., Speroni, F., Chapleau, N., de Lamballerie, M., Anon, M.C., and Anton, M., *Effect of high-pressure treatment on emulsifying properties of soybean proteins*. Food Hydrocolloids, 2005. **19**: p. 289-296.
85. Bengoechea, C., Jones, O.G., Guerrero, A., and McClements, D.J., *Formation and characterization of lactoferrin/pectin electrostatic complexes: Impact of composition, pH, and thermal treatment*. Food Hydrocolloids, 2011. **25**: p. 1227-1232.
86. Dukhin, A.S. and Goetz, P.J., *Characterization of aggregation phenomena by means of acoustic and electroacoustic spectroscopy*. Colloids and Surfaces A, 1998. **144**: p. 49-58.
87. Schneider, C., Hanisch, M., Wedel, B., Jusufi, A., and Ballauff, M., *Experimental study of electrostatically stabilized colloidal particles: Colloidal stability and charge reversal*. Journal of Colloid and Interface Science, 2011. **358**: p. 62-67.